國立臺灣大學工學院化學工程學研究所

碩士論文

Department of Chemical Engineering

College of Engineering

National Taiwan University

Master's Thesis

聚丁二烯批次製程之動態建模以及溫度控制

Dynamic Modeling and Temperature Control of PBL Emulsion Polymerization Batch Process

許秉祐

Ping Yu Hsu

指導教授：吳哲夫 博士

Advisor: Jeffrey D. Ward, Ph.D.

中華民國 113 年 7 月

July, 2024

doi:10.6342/NTU202402858

誌謝

能完成這篇論文，我要特別感謝我的指導教授吳哲夫與李豪業老師，也要感謝家人與朋友以及實驗室的每一位成員對我的支持與鼓勵，謝謝大家。

doi:10.6342/NTU202402858

中文摘要

聚丁二烯乳膠（PBL）是丙烯腈-丁二烯-苯乙烯共聚物（ABS）的共聚合過程中至關重要的組成部分，ABS 是一種廣泛使用的工業聚合物。然而，PBL 乳化聚合存在一些挑戰。除了本身反應的高放熱與單一操作批次間之黏度上升所造成的熱交換器熱傳效率降低之外，隨著操作批次次數的增加，熱交換器上所累積之聚合物結垢。這些因素都會導致潛在的溫度控制高超越比，進而導致不同批次之間的最終產品質量不一致。

為了解決這些問題，工程師通常會訴諸於人工調整控制器參數與製程變數。然而，這種方法由於操作人員經驗的差異而缺乏一致性，導致生產力和產品質量不可預測。

本研究針對於聚丁二烯乳化聚合批次製程相關的挑戰進行探討。通過開發能夠捕捉實際工廠動態的數學模型，進而優化製程生產力與控制策略並保持不同批次之間的一致產品質量。

doi:10.6342/NTU202402858

ABSTRACT

Polybutadiene Latex (PBL) is a crucial component in the copolymerization process for Acrylonitrile Butadiene Styrene (ABS), a widely used industrial polymer. However, the control of PBL emulsion polymerization reactors are particularly difficult due to the multiphase nature of emulsion systems and the complicated nonlinear process dynamics[39].

To address these issues, engineers often resort to manual adjustments of process parameters. However, this approach suffers from inconsistencies due to variations in individual operating experience, leading to unpredictable productivity and product quality.

This research addresses the challenges associated with polybutadiene emulsion polymerization, including exothermic reactions, increasing viscosity within each batch operation, and polymeric fouling accumulates on heat exchangers across batches. These factors contribute to potential temperature control overshoots, resulting in inconsistent final product quality across different batches.

By developing a mathematical model that captures real-plant dynamics, the research seeks to optimize productivity, control strategy and maintain consistent product quality across batches.

doi:10.6342/NTU202402858

CONTENTS

doi:10.6342/NTU202402858

doi:10.6342/NTU202402858

LIST OF FIGURES

doi:10.6342/NTU202402858

doi:10.6342/NTU202402858

doi:10.6342/NTU202402858

LIST OF TABLES

doi:10.6342/NTU202402858

Chapter 1 Introduction

1.1 Research Background

Due to the ever-increasing computational power of computers, mathematical modeling has become a ubiquitous practice across all engineering disciplines. This is particularly true in chemical engineering, where real-plant experimentation can be impractical due to high risks and significant economic costs. Consequently, developing simulation models that accurately capture real-plant dynamics and responses has become a crucial area of study.

These models offer a valuable tool for process development. Researchers can use them to experiment with control structures, optimization strategies, and process time minimization, ultimately leading to cost reductions. With these objectives in mind, this thesis aims to present a mathematical model capable of capturing the behavior and real-time responses during polybutadiene production. The model will then be used to explore and optimize control strategies beforehand.

1.2 Process Description

This study adopts the process from Yeo et al.(2004) [1], Figure 1-1 shows the schematics of the PBL reactor considered in the present study. The process involves heating the reactor to a specific temperature, followed by initiator injection. Liquid ammonia ($NH_{3,liq}$) circulating through the heat exchange tubes within the reactor acts as a refrigerant to remove the heat generated during the reaction. The reactor temperature is

doi:10.6342/NTU202402858

controlled by adjusting the refrigerant level within the heat exchange tubes.

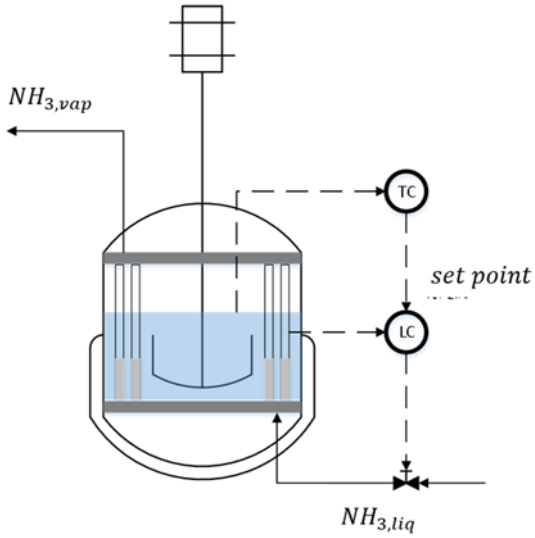

Figure 1-1 Schematics of the PBL reactor

Figure 1-2 shows the control structure of the PBL reactor, the control structure is a typical cascade control system. The primary controller (G_{c1}) determines the refrigerant level set point for the secondary controller (G_{c2}) by comparing the real time reactor temperature with the reactor temperature set point. The secondary controller controls the refrigerant level by manipulating the valve position of the refrigerant.

In Figure 1-2 G_{P1} represents the dynamic characteristics of the reactor temperature responses to the change in refrigerant level within the heat exchange tubes. Similarly, G_{P2} describes the dynamic behavior of the refrigerant level itself in response to adjustments in valve position .

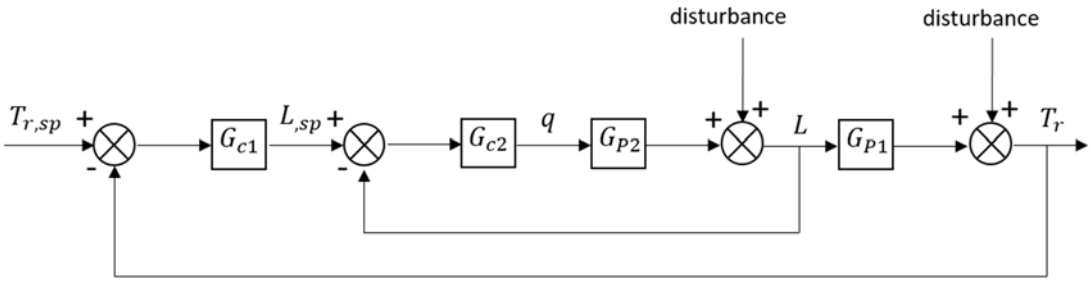

Figure 1-2 Block diagram of the PBL reactor control system

doi:10.6342/NTU202402858

1.3 Research Objectives

This research aims to develop a first principles mathematical model that captures the dynamic behavior of non-isothermal emulsion polymerization of polybutadiene (PBL) within a batch reactor. This model will serve as a tool to investigate and optimize the polymerization process. Specifically, we will leverage the model to explore two key objectives: maximizing productivity (which translates to minimizing batch operation time) and identifying the optimal control strategy for the reactor temperature profile.

doi:10.6342/NTU202402858

Chapter 2 Literature Review

2.1 Reaction Temperature Effect on PBL

Polybutadiene latex (PBL) is a synthetic polymer produced via free radical polymerization of butadiene (BD) within an emulsion system. Variations in reaction temperature during this free radical emulsion polymerization process can influence the isomeric structure of the resulting polybutadiene[2], ultimately leading to differences in the final product's particle size distribution.

Condon 1953[2] investigated the influence of the temperature of polymerization on the structural composition of emulsion polymers of butadiene and discussed the presence of a maximum in the percentage of vinyl double bonds in the polymer, which was previously thought to be due to gelation but is actually inherent to the polymerization system involving three competing modes.

Pires 2004[3] employed a experiment that shows that the conversion of butadiene monomer is significantly influenced by the reaction temperature, the results suggest that there’s an optimal reaction temperature exists between 70°C and 80°C. Reaction temperatures exceeding this range will trigger a rapid increase in reaction rate, potentially leading to temperature overshoot.

2.2 Reactor pressure of PBL production

Meehan (1949)[4] investigated the relationship between monomer pressure and conversion in butadiene emulsion polymerization. Their study revealed that the

doi:10.6342/NTU202402858

polymer-solvent system in emulsion polymerization does not conform to Raoult's law. Additionally, they observed that butadiene pressure starts to decline at a conversion of approximately 52% and that the timing of this decline is independent of both emulsifier concentration and reaction temperature. The study confirmed that the abrupt drop in system pressure is directly related to the disappearance of the monomer dispersed phase. This suggests that hydrophobic monomers initially form a dispersed oil phase during the polymerization reaction, and that the unreacted monomer oil phase is completely dissolved into the polymer particles as the reaction progresses. Furthermore, it was found that the amount of butadiene dissolved in polybutadiene is not affected by latex particle size but only by the number of polymer molecules. The solubility of butadiene-polybutadiene does not change significantly with temperature.

2.3 General Features of Emulsion Polymerization

The formulation of emulsion polymerization typically includes monomer, water, surfactant, and a water-soluble initiator. Monomer droplets, micelles, and particle nuclei play essential roles in the polymerization process, with the initiation reaction leading to the formation and growth of polymer particles in the aqueous phase.

Emulsion polymerization is a process where free radicals react with monomer molecules in discrete polymer particles dispersed in an aqueous phase, typically ranging from 10^{16} to 10^{18} particles per cubic meter, impacting the properties of latex products.

According to the nucleation model proposed by Harkins ([11] - [13]) and Smith ([14] - [16]), we can know that the latex particles are produced mainly by micelles capturing the free radicals in the water-oil interface. The monomer droplets can not

doi:10.6342/NTU202402858

capture the free radicals effectively due to its small surface area.

The typical emulsion polymerization includes three intervals, the first interval is the nucleation of the monomer-swollen-micelles. It involves the initiation of polymerization reactions within micelles that have absorbed monomer molecules, leading to the formation of primary polymer particles dispersed in the continuous aqueous phase.

The second interval is the growth of latex particles, This growth period involves the propagation reaction of free radicals with monomer molecules at the particle-water interface, leading to the expansion of polymer particles.

The third interval is the consumption of residual monomer, the reaction proceeds from second interval to third interval when all the dispersed monomer droplets are disappear in the continuous aqueous phase.

doi:10.6342/NTU202402858

Chapter 3 Process Model Development

This chapter delves into the process model development for this research. It provides a detailed description of the equations and parameters used to model the reactor within the process. Additionally, it explores the intricacies of the emulsion polymerization mechanism, going beyond the typical free radical polymerization modeling approach.

The process model was developed using the Scilab Xcos simulation environment. A detailed process diagram of the model can be found in Appendix B, and the model parameters are provided in Appendix C.

3.1 Modeling of Reactor Temperature Trajectory

The simulation of the reactor temperature trajectory is achieved by implementing an energy balance equation (see Equation 3-1). This equation captures the heat transfer within the reactor. To achieve the desired reaction temperature, steam is directly injected into the reactor. The heat released during steam condensation then serves to heat the reaction mixture.

$$\frac{d}{dt}\left(T_r * V_r * \rho_r * C_{pr}\right) = \left(R_p * \Delta H_p\right) * V_r - UA_{tubes} * (T_r - T_{tube}) + \dot{m}\,(C_{p_{steam}} * (T_{steam} - T_{reactor}) + H_{v_{steam}}) \quad 3\text{-}1$$

T_r = rector temperature [K]

T_{tube} = temperature of the heat exchange tubes [K]

T_{steam} = temperature of the heating steam [K]

doi:10.6342/NTU202402858

V_r = reactor volume [m^3]

UA_{tubes} = overall heat transfer coefficient of the heat exchange tubes [$\frac{W}{K}$]

$reaction\ heat = R_p * \Delta H_p$ [$\frac{kJ}{min}$]

ΔH_p = heat of polymerization [$\frac{J}{mol}$]

$\dot{m}$ = mass flow rate of steam injection [$\frac{kg}{min}$]

$H_{v_{steam}}$ = condensation heat of the heating steam [$\frac{J}{mol}$]

ρ_r, V_r, C_{pr} = reactant density [$\frac{kg}{m^3}$], volume[m^3] and heat capacity [$\frac{J}{kg*K}$]

3.2 Modeling of Heat Exchange Tubes

The reactor temperature is maintained by regulating the liquid level of the refrigerant (liquid ammonia) within the heat exchange tube. A mass balance equation is employed to simulate the dynamic changes in the liquid level (see Equation 3-2).

The heat exchange tubes are configured as cylinders (see Figure 3-1). Details regarding their material and dimensions are provided in the Appendix. Liquid ammonia is pumped through a valve (the valve characteristic is given in Appendix A) and evenly distributed within the tubes, where it absorbs the reaction heat through vaporization. Note that the temperature of the heat exchange tube is constant, same with the saturated temperature of the liquid ammonia.

To simplify the model further, this research assumes a uniform liquid ammonia level within all the heat exchange tubes at any given time.

doi:10.6342/NTU202402858

$$\frac{dH_{liq}}{dt} = \frac{Q_v}{A_{c,tube} * n_{tube}} - U_{tube} * 2\pi r_i * H_{liq} * \frac{(T_r - T_{tube})}{\frac{\Delta H_{vap}}{MW_{NH_3}} * A_{c,tube} * \rho_{NH_3}} \quad 3\text{-}2$$

H_{liq} = liquid level of the refrigerant within the heat exchnge tube [m]

$U_{tube} = \frac{1}{U_{tube}} = \frac{1}{h_i} + \frac{tube\ thickness}{k} + \frac{1}{h_o}$ $[\frac{W}{m^2 * K}]$

ΔH_{vap} = vaporization heat of ammonia $[\frac{J}{mol}]$

MW_{NH_3} = molecular weight of liquid ammonia $[\frac{kg}{mol}]$

Q_v = volumetric flow rate flow through the valve $\left[\frac{m^3}{s}\right]$

$A_{c,tube}$ = cross sectional area of the tube $[m^2]$

n_{tube} = number of the tubes

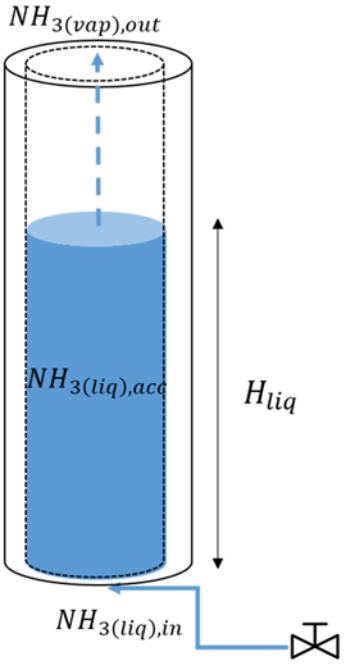

Figure 3-1 Configuration of a heat exchange tube

doi:10.6342/NTU202402858

3.3 Modeling of the Reactor Pressure

The reactor pressure is simulated by considering the combination of the vapor pressure of the water and the vapor phase butadiene monomer within the reactor. The Antoine equation (see Equation 3-3) is employed to calculate the individual vapor pressures. The parameters and thermodynamic data used in the equation were validated using Aspen Plus software (see Table 3-1, Figure 3-2 and Figure 3-3).

As noted in the literature review, the pressure within a batch reactor used for PBL production exhibits a decreasing trend.

The decrease in reactor pressure during the reaction is simulated using a critical monomer conversion approach. This approach assumes that the reactor pressure starts to drop once a critical value of monomer conversion (x_c) is reached (see Figure 3-4).

This is due to the disappearance of the monomer droplets in the liquid phase of the reactant. When the monomer droplet disappear, the monomer within the vapor phase will start to dissolve into the liquid phase which leading a reduction in the overall reactor pressure.

$$\ln p_i = c_{1,i} + \frac{c_{2,i}}{T + c3i} + c_{4,i} * T + c_{5,i} * lnT + c_{6,i} * T^{c_{7,i}} \quad (for\ c_{8,i} \le T \le c_{9,i}) \qquad 3\text{-}3$$

Table 3-1 Parameters of Antoine Equation by Aspen Plus

	$c_{1,i}$	$c_{2,i}$	$c_{3,i}$	$c_{4,i}$	$c_{5,i}$	$c_{6,i}$	$c_{7,i}$
Butadiene	64.0591	−4621.9	0	0	−8.5323	$1.2269 * 10^{-5}$	2
Water	62.1361	−7258.2	0	0	−7.3037	$4.1653 * 10^{-6}$	2

doi:10.6342/NTU202402858

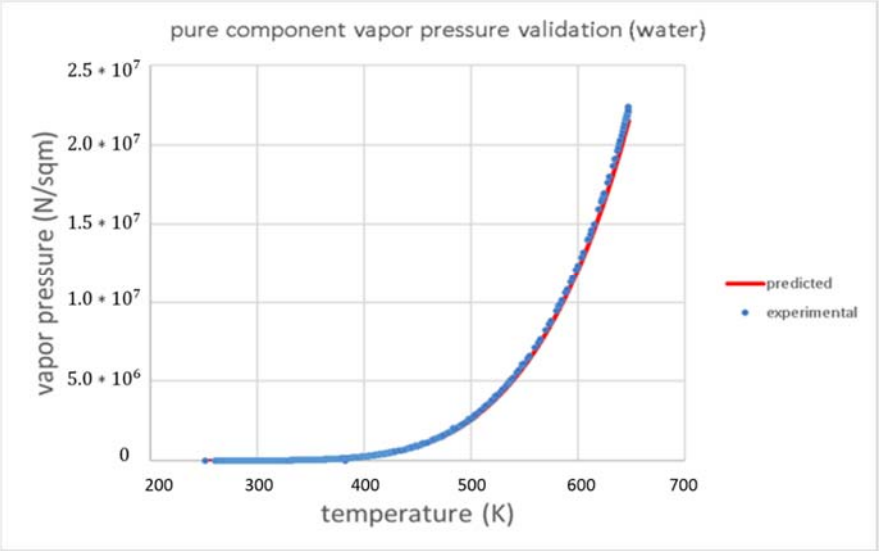

Figure 3-2 Thermodynamic validation of water by Aspen Plus

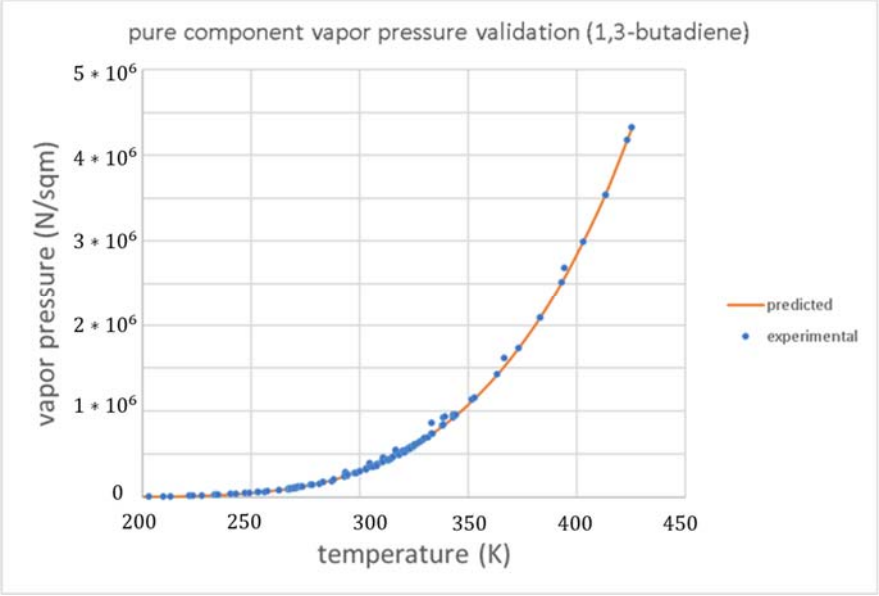

Figure 3-3 Thermodynamic validation of BD by Aspen Plus

doi:10.6342/NTU202402858

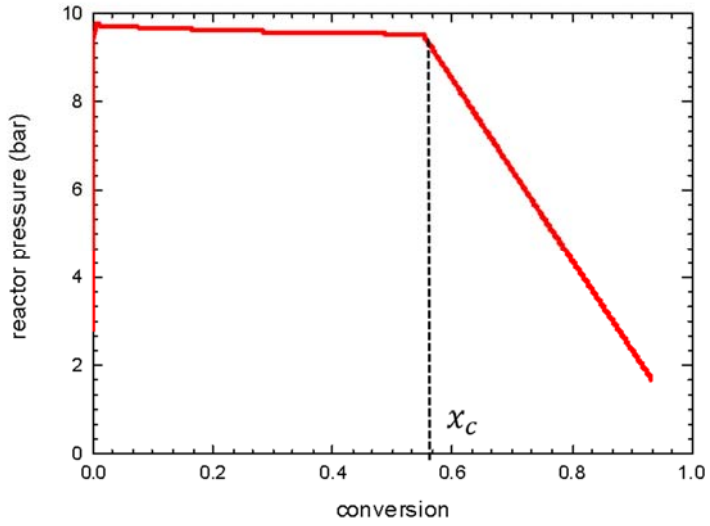

Figure 3-4 Typical profile of reactor pressure versus conversion.

3.4 Modeling of the Polymeric Fouling on Heat Exchange Tubes

Takamatsu et al. (1987)[7] described the decrease of the overall heat transfer coefficient in the polymerization batch reactor by using an empirical form correlation (see Equation 3-4).

$$U = U_0 * [1 - a * \exp\left(1 - \frac{1}{x_m}\right)] \qquad 3\text{-}4$$

Where x_m denotes the monomer conversion and U_0 is the value of the overall heat transfer coefficient of the heat exchange device at $x_m = 0$ (where there is no polymer in the reactor, see Appendix E for details), and the a is a constant parameter. Soroush and Costa (1992) [9] provided a modified form of the correlation to better capture the decline

doi:10.6342/NTU202402858

of the overall heat transfer coefficient in the polymerization batch reactor (see Equation 3-5).

$$U = U_0 \left(a + (1 - a) * \exp(-b * x_m^e) \right) \quad \text{3-5}$$

$a, b, e = \text{constant parameter} = 0.2, 7, 3$

However, the correlation proposed by Soroush and Costa (1992) predicts an unrealistic 80% decline in the overall heat transfer coefficient within a single batch cycle, which is different from typical industrial experience. In real-world plants, batch reactors typically undergo cleaning after 30 to 40 runs. To address this discrepancy and accurately represent the decrease in U both within a batch cycle and across multiple cycles, this research adopts and modifies the correlation from Equation 3-5. This approach utilizes two empirical correlations: one describing the decline in the heat transfer coefficient during a single batch (see Equation 3-6) and another capturing the cumulative effect across multiple batches.

$$U = U_{0,j} \left(0.6 + 0.4 * \exp(-7 * x_m^3) \right) \quad \text{3-6}$$

Here the subscript j indicates batch number $U_{0,1}$ denotes the initial value of the overall heat transfer coefficient at $x_m = 0$ during the first batch run, and the $U_{0,j}$ signifies the value of the overall heat transfer coefficient at the start ($x_m = 0$) of the $current$ batch run ($U_{0,batch\ number}$ takes into account the potential fouling effects accumulated from previous batches).

Equation 3-6 predicts a decrease of up to 40% in the overall heat transfer coefficient

doi:10.6342/NTU202402858

of the heat exchange tubes within each batch cycle.

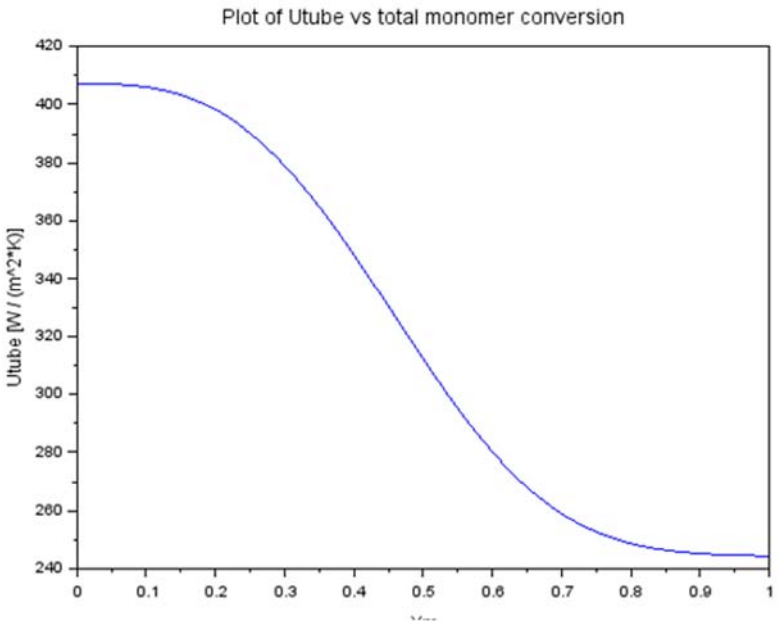

Figure 3-5 Demonstration of the fouling effect within each batch cycle

(y-axis : the overall heat transfer coefficient of the heat exchange tubes, x-axis : monomer conversion during the reaction)

Equation 3-7, on the other hand, suggests a cumulative decrease of up to 80% after 100 batch runs (see Figure 3-6).

$$U_{0,batch\ number} = U_0\ (\ 0.2 + (0.8) * \exp\left(-7 * \left(\frac{batch\ number}{100}\right)^3\right)) \qquad 3\text{-}7$$

doi:10.6342/NTU202402858

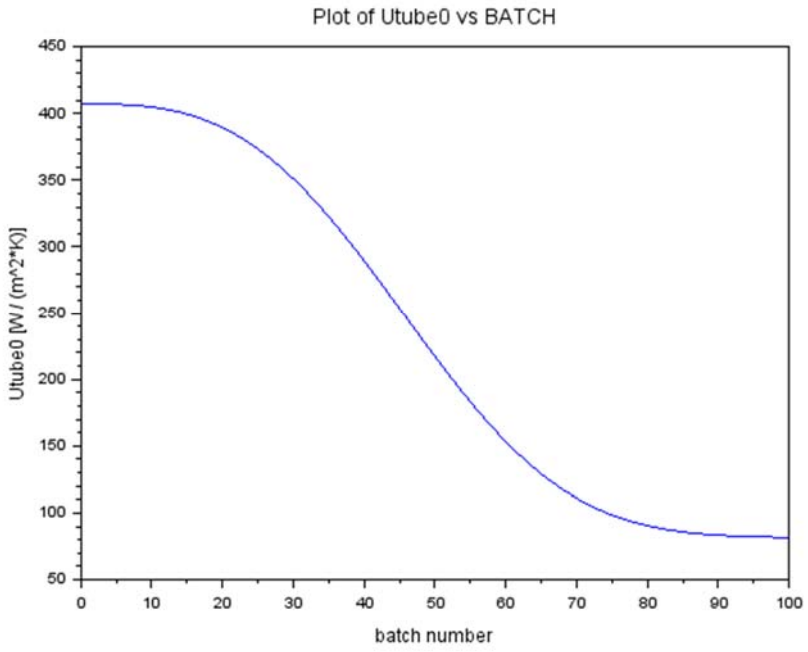

Figure 3-6 Demonstration of the fouling effect within 100 batch cycles

(y-axis : the initial value of the overall heat transfer coefficient of the heat exchange tubes, x-axis : number of batches)

3.5 Modeling of the Reaction Mechanism

Given that the focus of this research is on the temperature dynamics of the emulsion polymerization system, a simplified kinetic model and reaction mechanism were adopted. This model primarily captures the generation of reaction heat and the overall time-dependent monomer conversion within the reactor.

The model deliberately avoids describing the detailed chemical composition, molecular weight distribution, or particle size distribution of the system. Additionally, due to the changing volume of the reactant mixture in a batch system, employing moles of monomer instead of concentration simplifies the material balance calculations [8].

doi:10.6342/NTU202402858

While the specific characteristics of emulsion polymerization can vary depending on the reaction in question, a general form under the assumption of the Smith-Ewart case 2 [10] kinetics exists for describing the polymerization rate are:

$$R_p = k_P * C_{M,p} * \frac{n * N_p}{N_A} \qquad 3\text{-}8$$

where:

$R_p =$ polymerization rate $\left[\frac{\text{mol}}{s}\right]$

$k_P =$ propagation rate constant $[\frac{1}{s}]$

$C_{M,p} =$ monomer concentration within the particle phase $[\frac{mol}{m^3}]$

$n =$ number of free radicals per particle

$N_p =$ number of particle per unit volume of water $[1/m^3]$

$N_A =$ avogadra's constant $= 6.02 * 10^{23}$

To understand the nucleation mechanism of the reaction, the brief introduction of three intervals of the emulsion polymerization must be mentioned.

The reaction process initiates with the decomposition of initiator molecules in water, generating radicals. These radicals react with monomer molecules to form growing chains. Once a critical length is reached, the chains become insoluble in water and coil up to form particle nuclei. These unstable nuclei then aggregate and become stabilized by surfactant molecules, forming primary emulsion polymer particles. The above ideas can be described by the kinetic model developed by Fitch and Tsai [17]-[19] (see Equation 3-11).

To model the $C_{M,p}$ in the above equation, the critical monomer conversion approach [5] is employed to describe the decreasing characteristic of the monomer concentration

doi:10.6342/NTU202402858

within the particle phase of the reactant (see Equation 3-9 and Equation 3-10).

$$C_{M,p} = \frac{\rho_m}{MW_m} * \emptyset_M \qquad 3\text{-}9$$

where:

ρ_m = density of the monomer $[\frac{kg}{m^3}]$

MW_m = molecular weight of the monomer $[\frac{g}{mol}]$

$\emptyset_M$ = volumetric fraction of the monomer within the particle

$$\emptyset_M = \frac{1-x}{1-x * (1-\frac{\rho_M}{\rho_P})} \qquad 3\text{-}10$$

$x = x_c$ if $X \leq x_c$

$x = X$ if $X > x_c$

X = overall monomer conversion = $\frac{m_{\text{polymer}}}{m_{\text{monomer}} + m_{\text{polymer}}} \times 100\%$

x_c = critical monomer conversion

m_{polymer} = total moles of the polymer

m_{monomer} = total moles of the monomer

ρ_M = density of the monomer $[\frac{kg}{m^3}]$

ρ_P = density of the polymer $[\frac{kg}{m^3}]$

$$N_p = 0.37 * \left(\frac{\text{radical generation rate}}{\text{particle volume growth rate}}\right)^{0.4} (a_s * [E])^{0.6} \qquad 3\text{-}11$$

a_s = surface area occupid by emulsifier $[\frac{m^2}{kmol}]$

$[E]$ = emulsifier concentration $[\frac{kmol}{m^3}]$

doi:10.6342/NTU202402858

radical generation rate $= 2 * \mathrm{f} * k_d * [I]$

particle volume growth rate $= \frac{d}{dt}(\frac{m_P}{\rho_P * (1-\emptyset_m)})$

The purposes of modeling the consumption rate of the monomer is to simulate the heat generation during the reaction and to calculate the approximate conversion of the monomer, since that the monomer is consumed mostly in the propagation stage of the emulsion polymerization reaction. The consumption rate of the monomer is then employed as the negative value of the polymerization rate of the reaction.

$$\frac{dC_{M,R}}{dt} = -k_P * C_{M,p} * \frac{n * N_p}{N_A} \qquad 3\text{-}12$$

$C_{M,R} =$ total moles of monomer

3.6 Summary of the Model Assumptions

To achieve a balance between model simplicity, accuracy, and computational efficiency, several assumptions were made during the development of the mathematical model:

- Perfect mixing :

The stirred-tank batch reactor is modeled as a perfectly mixed system, which implies that the temperature, composition, and concentration are assumed to be uniform throughout the reactor volume at any given time.

This idealization simplifies the mathematical description of the system but may not

doi:10.6342/NTU202402858

perfectly capture potential localized variations that might occur in real-world reactors.

- All the particles are growing at the same rate (monodisperse) :

The system is assumed to exhibit monodisperse particle growth. This implies that all the polymer particles within the reactor have a uniform size distribution. In simpler terms, all particles form at the same time and grow at the same rate, resulting in a population of particles with identical diameters.

- Radicals can only be captured from the aqueous phase
- Smith-Ewart case 2 kinetic is applied (see Table 3-2) :

This assumption assumes that at any moment, the number of free radicals contain by the particle is either 1 or 0 (also known as zero to one model, see Figure 3-7), and the concentration of the monomer within the particle does not vary with reaction progress when monomer droplets are still present (the critical conversion approach). The Smith-Ewart kinetics has been proved to correctly describe the behavior of the emulsion polymerization of the relatively water insoluble monomer, such as styrene and butadiene[10].

Table 3-2 Smith-Ewart kinetic model assumptions [10]

The Smith-Ewart kinetic model is based on these following assumptions
1. Coagulation of particles do not occur and the number of particles per unit volume of water remains constant during polymerization.
2. Desorption of free radicals out of the particles does not take place.
3. Bimolecular termination of the polymeric radical inside the particle upon the entry of an oligomeric radical from the aqueous phase is instantaneous
4. The particle size distribution is relatively monodisperse

doi:10.6342/NTU202402858

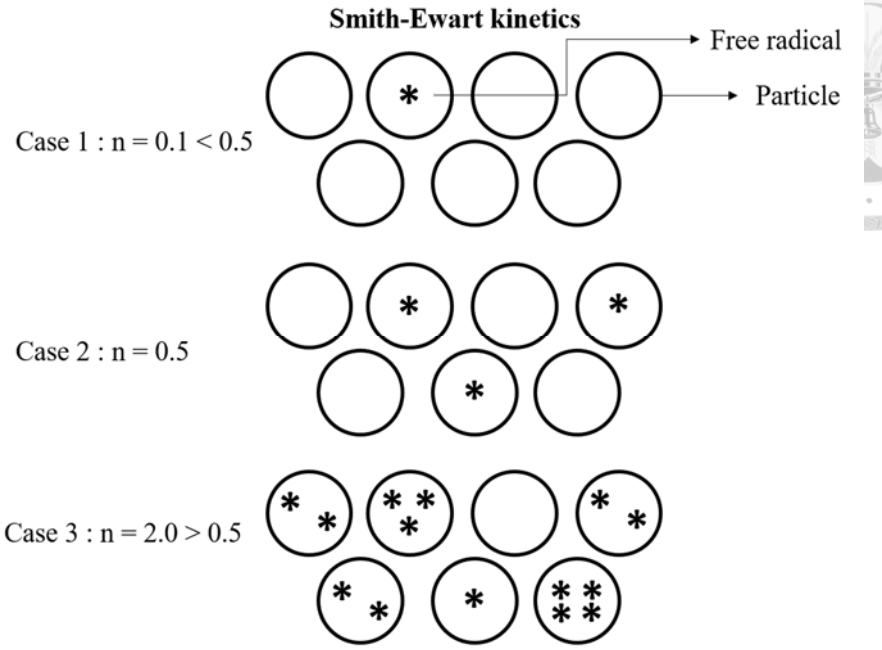

Figure 3-7 Schematic representation of Smith-Ewart kinetic

- Negligible mass transfer limitations for propagation, initiation, and termination reactions
- All the monomer is consumed during the propagation stage
- All the reactions are assumed to be 1st order reactions, which is a usual assumption for describing an impurity-free free radical polymerization system [5].

doi:10.6342/NTU202402858

Chapter 4 Model testing

4.1 Three Stages Heating Process

The reactor temperature trajectory adopted in this research has three stages, similar to the approach employed by Yeo et al. (2004) [1] (see Figure 4-1 and Table 4-1).

The process begins with heating the reactor to the desired reaction temperature of 333 K using direct steam injection. Once the target temperature is reached, the steam injection stops and the reaction is initiated by introducing the initiator.

It's important to note that direct steam injection is only used for the initial heating phase, raising the reactor temperature from 298 K to 333 K. Subsequently, the exothermic nature of the reaction itself provides all the necessary heat for further temperature increases.

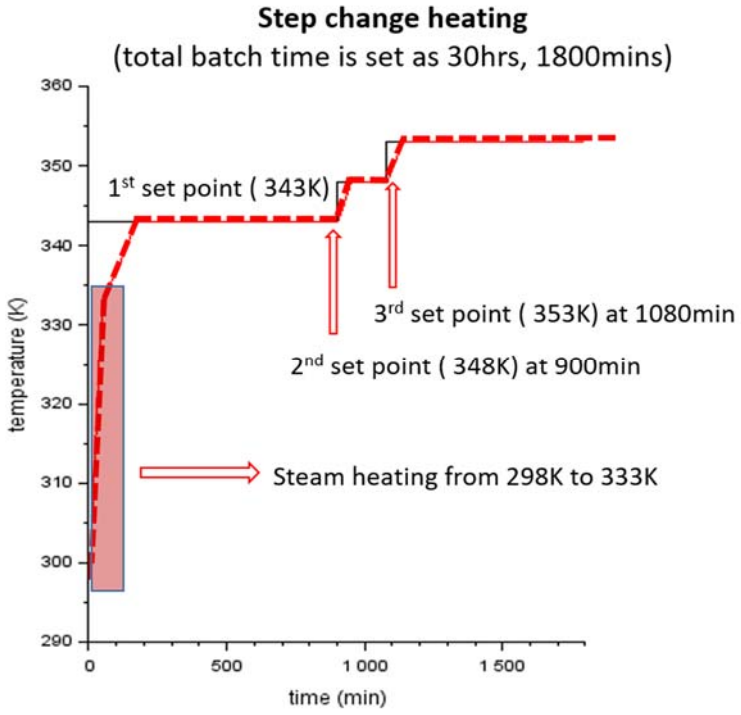

Figure 4-1 Three-stage step change of the reactor temperature set point

doi:10.6342/NTU202402858

Table 4-1 Three-stage ram change heating progress

Progress	Temperature (K)	Time duration
1st heating stage (steam)	298 K → 333 K	1.5 hours
1st heating stage (reaction heat)	333 K → 343 K	1.5 hours
1st isothermal stage	343 K	12 hours
2nd heating stage	343 K → 348K	1 hour
2nd isothermal stage	348 K	2 hours
3rd heating stage	348 K → 353 K	1 hour
3rd isothermal stage	353 K	11 hours

The purpose of having a three-stage step change heating process is to raise up the reactor temperature as fast as possible without violating the reactor pressure limitation for safety issues.

The reactor pressure is primarily attributed to the combined contributions of two components: the saturated vapor pressure of the butadiene monomer and the water present in the vapor phase. Notably, the butadiene monomer accounts for over 90% of the total reactor pressure.

Ideally, the reactor pressure will be a constant value within the 1st isothermal stage of the three-stage heating process. The reactor will only begin to drop after the reaction reaching the critical monomer conversion, when the monomer droplets within the aqueous phase disappear and the butadiene monomer within the vapor phase starts getting consumed.

It is important to keep the temperature set point of the 1st stage of the heating process low enough so that the reactor pressure limitation will not be violated, and raise the reactor temperature to the desired temperature as quickly as possible to shortening the

doi:10.6342/NTU202402858

batch time.

4.2 Noise-Free Model

The following plots depict the simulated trajectories for the 1st, 30th, and 45th batch runs (see Figure 4-2~Figure 4-7). The implemented control structure is same as that of the LG process [1] (see Figure 1-2), with a PI controller as the primary controller ($K_c = 1\frac{\%}{\%}, \tau_I =$ 20min) and a P-only controller as the secondary controller ($K_c = 5\frac{\%}{\%}$) . The controller parameters shown above were adopted and modified from the LG process [1] and used as a default setting. The results reveal a progressive accumulation of polymer fouling on the heat exchange tubes as the number of batches increases.

This polymeric fouling issue leads to a decline in the overall heat transfer coefficient. Consequently, maintaining reactor temperature becomes more challenging, as indicated by the increasing overshoot as the controller reaches saturation (see Figure 4-2 and Figure 4-4).

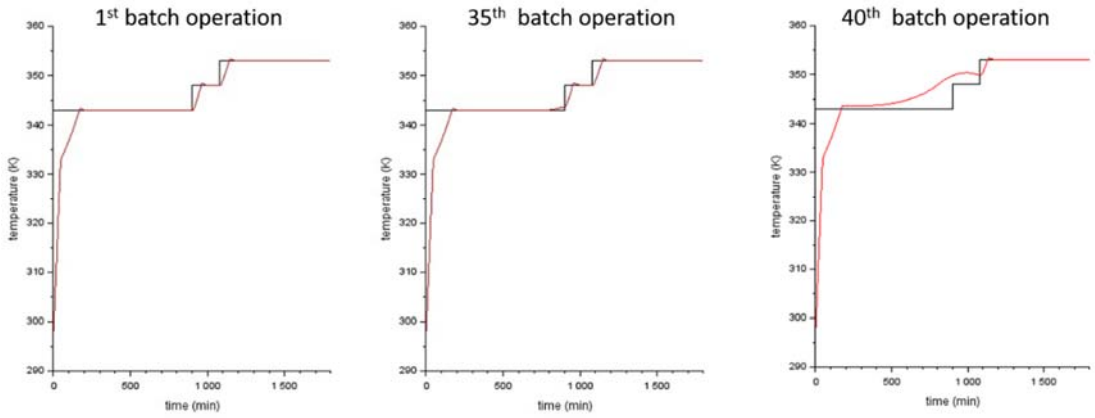

Figure 4-2 Reactor temperature trajectories (**red line** : reactor temperature [K], **black line** : reactor temperature set point [K])

doi:10.6342/NTU202402858

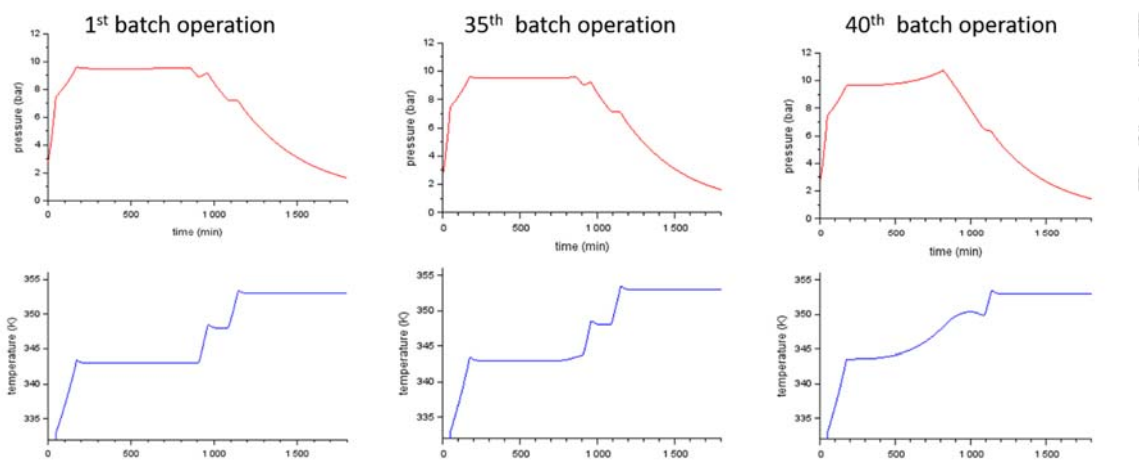

Figure 4-3 Reactor pressure and temperature trajectories (**red line** : reactor pressure [bar], **blue line** : reactor temperature [K])

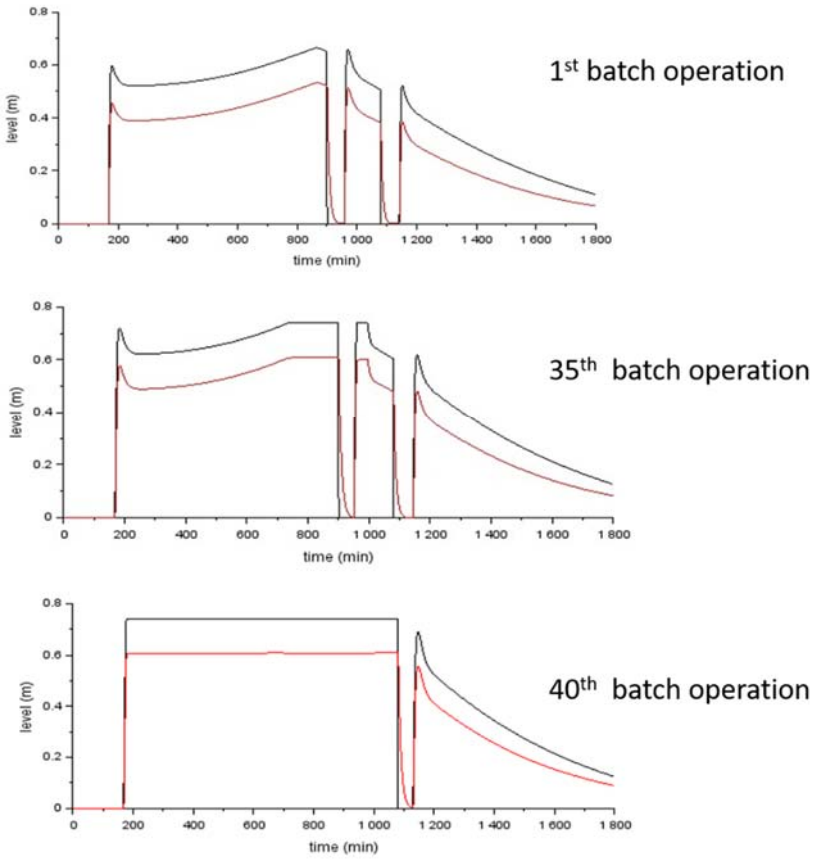

Figure 4-4 Refrigerant liquid level trajectories (**red line** : refrigerant liquid level [m], **black line** : refrigerant liquid level set point [m])

doi:10.6342/NTU202402858

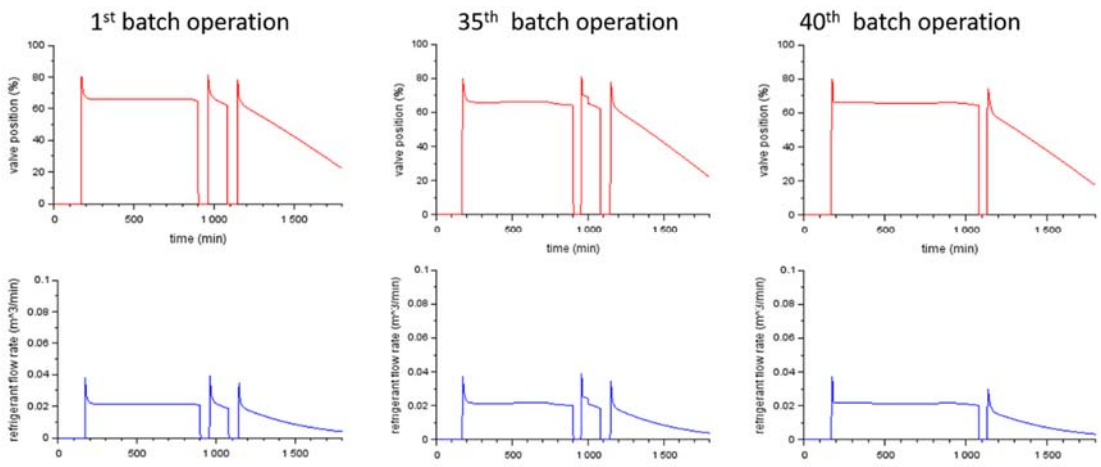

Figure 4-5 Valve position and refrigerant flow rate trajectories (**red line** : valve position [%], **blue line** : refrigerant flow rate [$\frac{m^3}{min}$])

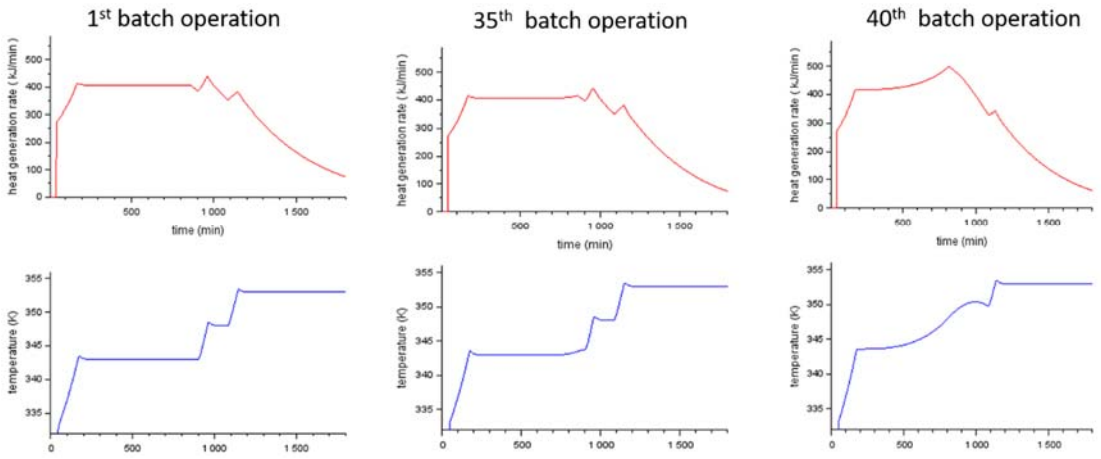

Figure 4-6 Reaction heat generation and reactor temperature trajectories (**red line** : reaction heat generation ($\frac{\text{kJ}}{min}$), **blue line** : reactor temperature (K))

doi:10.6342/NTU202402858

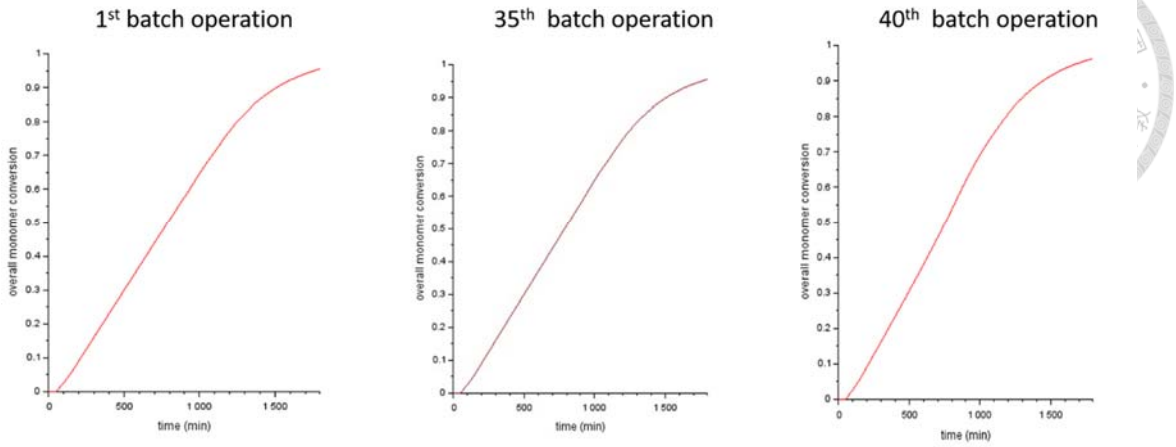

Figure 4-7 Overall monomer conversion trajectories

The dynamic responses are different from the real-plant operation dynamics published by [1] . However, even without complete knowledge of the actual process, we can still analyze the real plant data using fundamental control principles.

The observed significant drops in the real-plant reactor temperature trajectory suggest potential uncontrolled cooling events during the batch process. These drops could be indicative of additional feeds being introduced to the reactor. The oscillatory behavior observed in the reactor temperature trajectory is most likely be caused by the controller and the measurement noise in the reactor temperature sensor.

4.3 Sensitivity Analysis of the Process Noise

Real-plant operations sometimes experience measurement noise, leading to oscillatory behavior in the control loop. To make the model more realistic and capture potential real-world process variations, sensitivity analyses of process noise were also conducted. There are several common sources of process noise, such as temperature measurement noise, level measurement noise and valve position measurement noise.

doi:10.6342/NTU202402858

Unlike the smooth line predicted by the mathematical equations, the actual reaction heat generation trajectory in the real process will exhibit deviations and fluctuations.

To generate the noisy data, white noise is introduced to the process model. Specifically, measurement noise was generated from uniform distribution in the range of $0.5 \sim -0.5$ [K] for the reactor temperature, $0 \sim 10\%$ for the refrigerant level within the heat exchange tubes and $10\% \sim -10\%$ for the refrigerant valve position and the reaction heat generation.

The sudden drop during the first isothermal stage in the real plant operation is also considered in the modified process model with the implementation of a step change to the reactor temperature (see Appendix B).

The impact of these different noises on the process model are shown as the following simulation results (see Figure 4-8 ~ Figure 4-11).The simulation results (shown below) demonstrate that introducing white noise into the temperature measurement can significantly impact the temperature profile.

doi:10.6342/NTU202402858

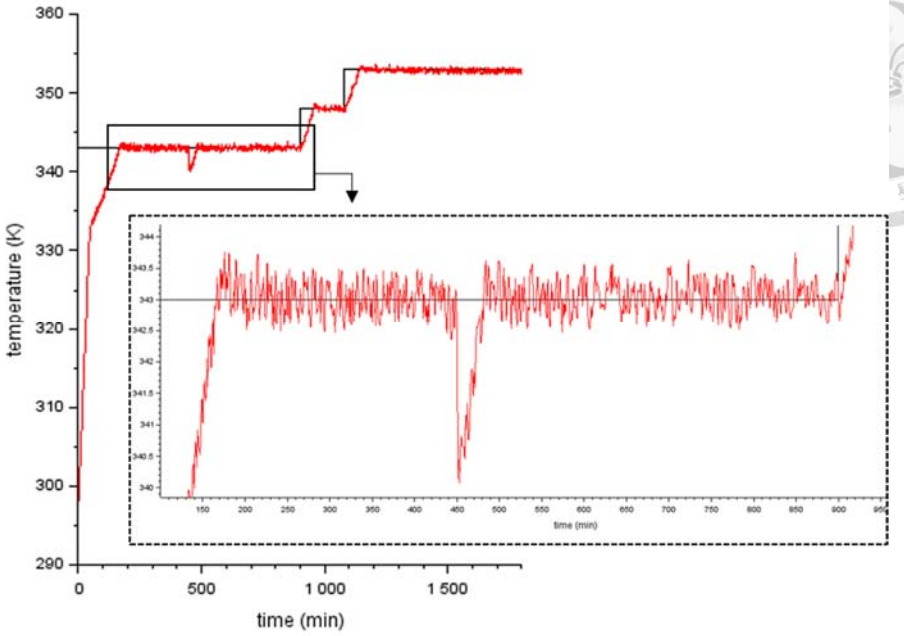

Figure 4-8 1st batch reactor temperature trajectory with temperature measurement noise only(**red line** : reactor temperature [K], **black line** : reactor temperature set point [K])

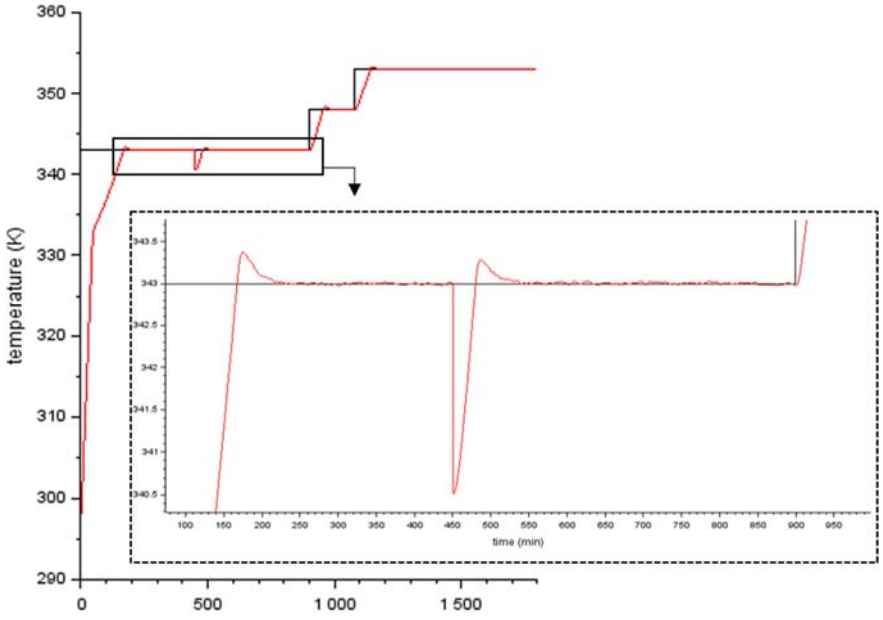

Figure 4-9 1st batch reactor temperature trajectory with level measurement noise only (**red line** : reactor temperature [K], **black line** : reactor temperature set point [K])

doi:10.6342/NTU202402858

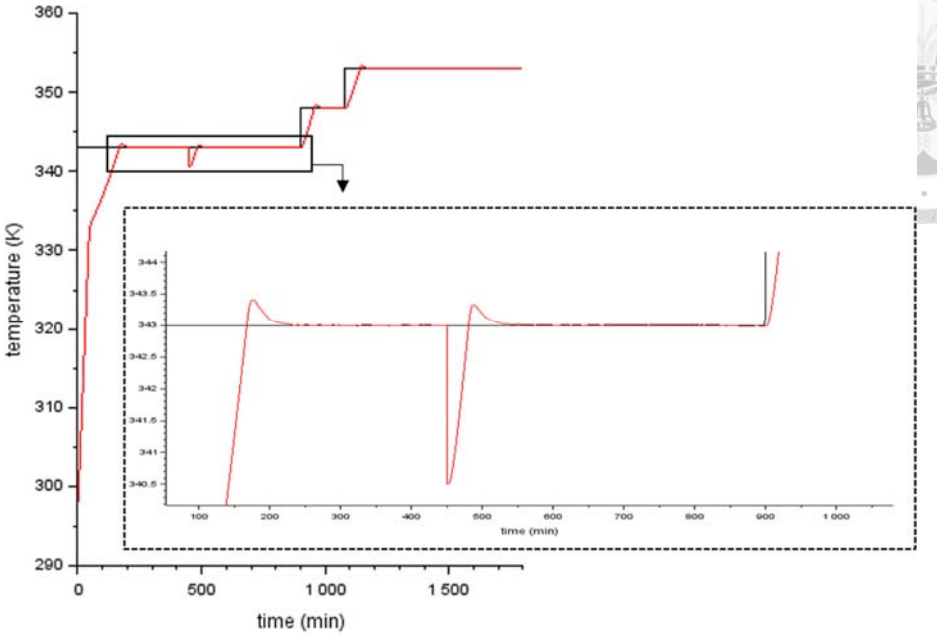

Figure 4-10 1st batch reactor temperature trajectory with valve measurement noise only

(**red line** : reactor temperature [K], **black line** : reactor temperature set point [K])

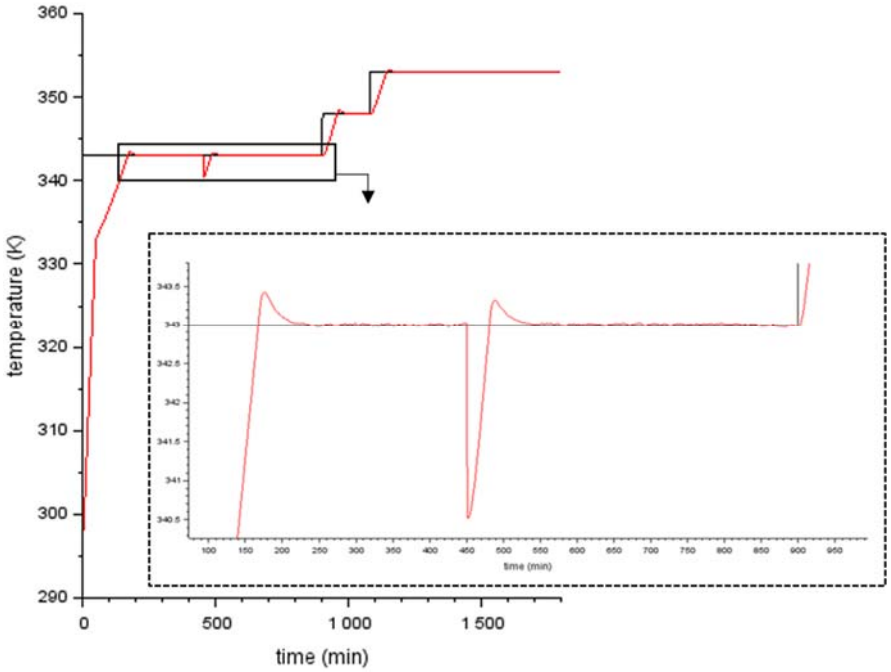

Figure 4-11 1st batch reactor temperature trajectory with heat generation noise only

(**red line** : reactor temperature [K], **black line** : reactor temperature set point [K])

doi:10.6342/NTU202402858

Real-world plant operation data shows fluctuations in refrigerant level and flow rate. These fluctuations exhibit a lower frequency compared to the white noise used in this work. To replicate this characteristic in the simulation, a sine wave is introduced as noise into the measurements of both refrigerant liquid level and flow rate.

The simulation results of the reactor temperature, refrigerant liquid level and valve position trajectories with only the implementation of the sine wave noise are shown below (see Figure 4-12 ~ Figure 4-14).

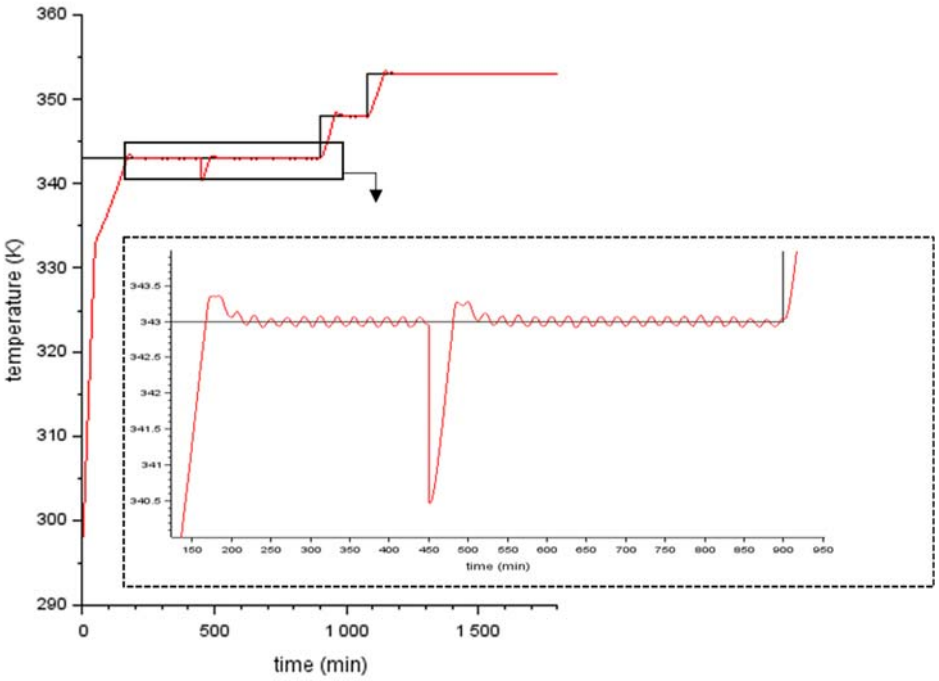

Figure 4-12 1st batch reactor temperature trajectory with sine wave noise in level and valve measurement only (**red line** : reactor temperature [K], **black line** : reactor temperature set point [K])

doi:10.6342/NTU202402858

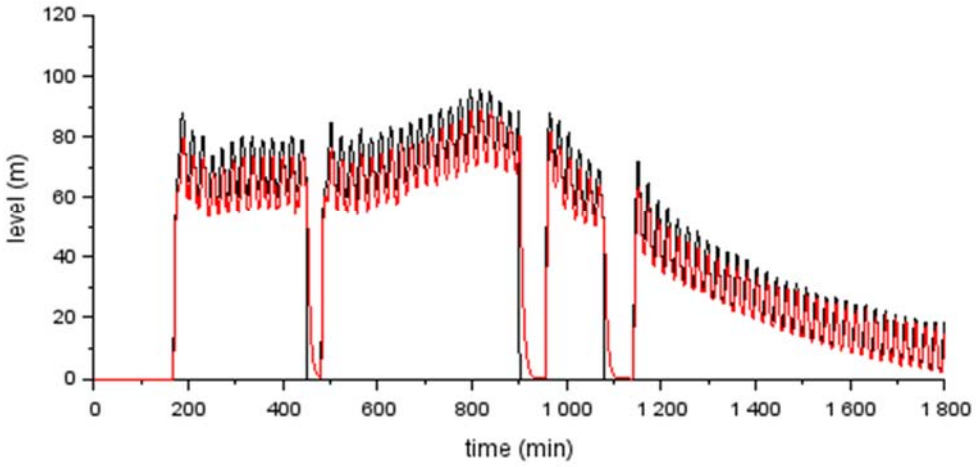

Figure 4-13 1st batch refrigerant liquid level trajectory with sine wave noise in level and valve measurement only (**red line** : refrigerant liquid level [m], **black line** : refrigerant liquid level set point [m])

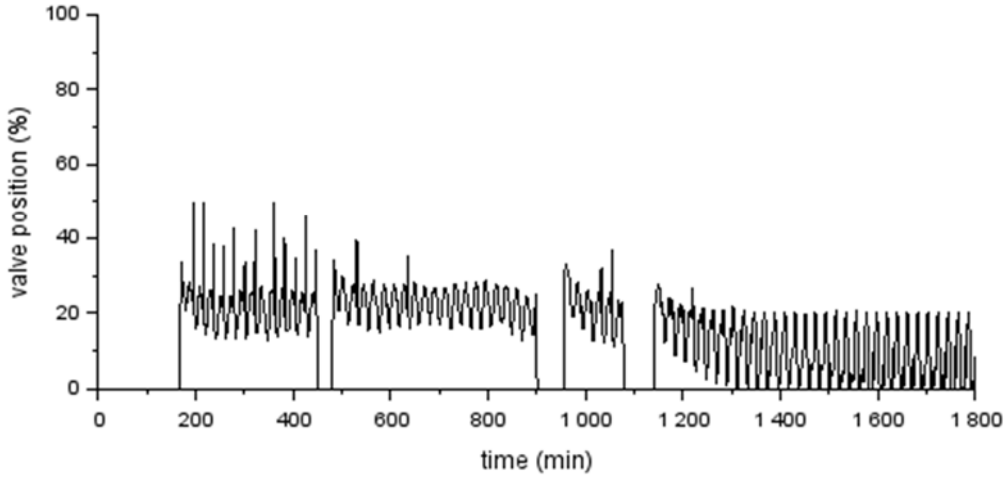

Figure 4-14 1st batch refrigerant valve position trajectory with sine wave noise in level and valve measurement only

This simulation model includes noise to represent the random and regular fluctuations observed in a real-world reactor system. White noise, with its unpredictable

doi:10.6342/NTU202402858

variations, is added to the measurement of the reactor temperature to mimic the inherent uncertainties present in the actual process. For the refrigerant level and flow rate measurement, sine wave noise is introduced to simulate the characteristic, lower-frequency oscillations seen in these measurements. This combined approach allows the model to capture both the unpredictable and somewhat regular disturbances that occur during real-world reactor operation.

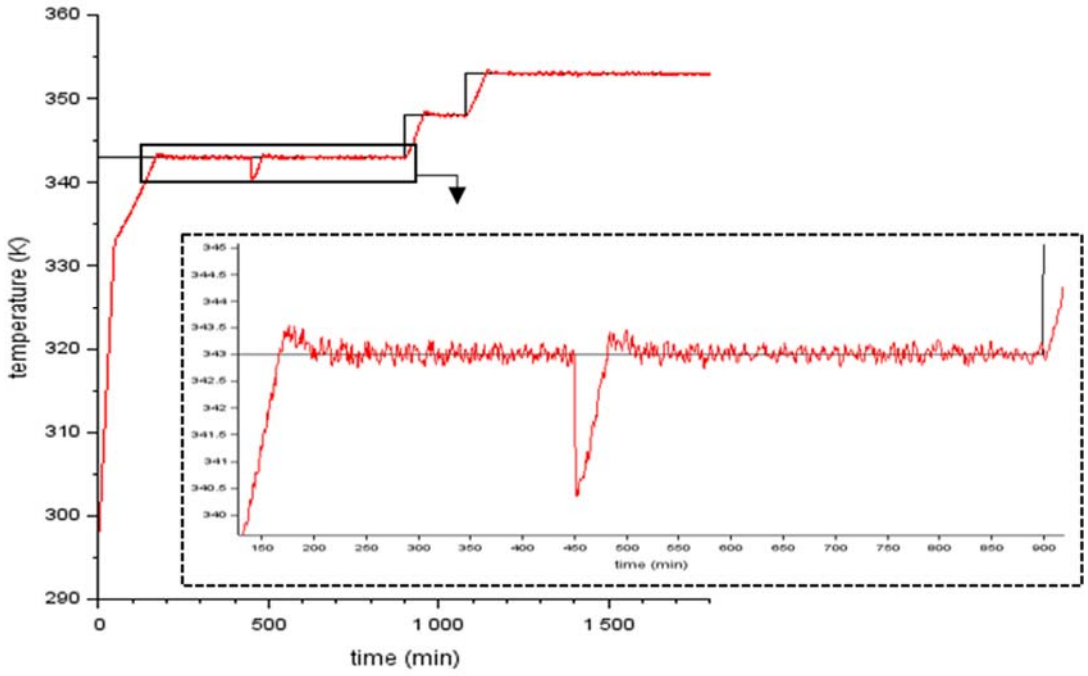

Figure 4-15 1st batch reactor temperature trajectory with all the noise (**red line** : reactor temperature [K], **black line** : reactor temperature set point [K])

doi:10.6342/NTU202402858

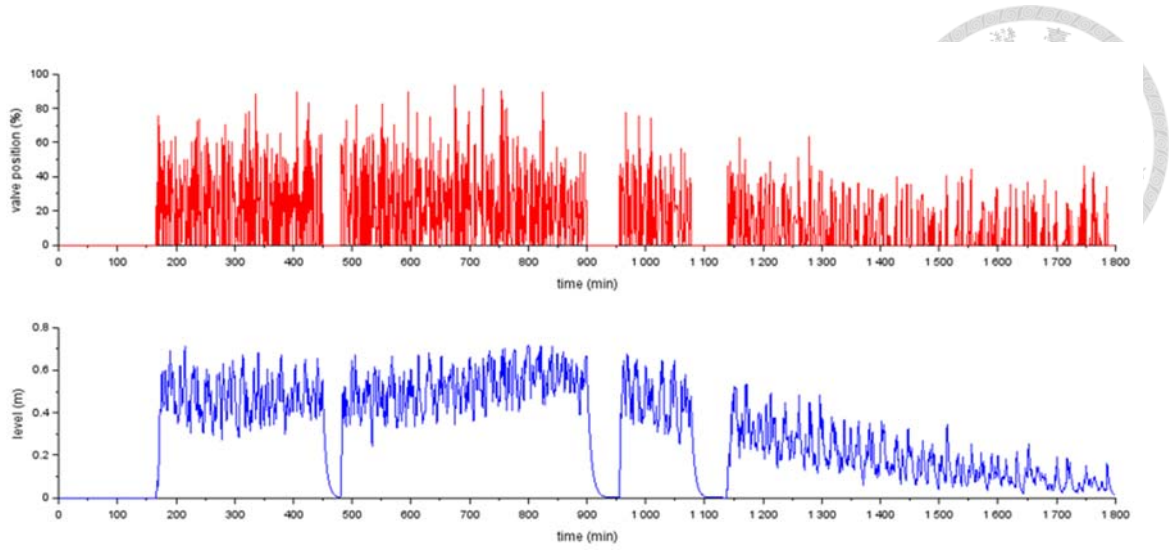

Figure 4-16 1st batch refrigerant valve position and level trajectory with all the noise

doi:10.6342/NTU202402858

Chapter 5 Process optimization

5.1 Optimal Temperature Profile

Because maximizing batch productivity is equivalent to minimizing the batch operation time, one of the critical steps of developing a dynamic process model is to determine the time-optimal temperature profile for a given initial condition, ensuring that the polymer achieves the desired level of monomer conversion [21].

The challenge of finding the time-optimal temperature profile for polymerization reactions has been addressed by several researchers. Masterson (1977) [22] and Chen (1978) [23] employed the maximum principle to solve this minimum time problem for batch reactors involving styrene polymerization. Wu et al. (1980) [24] presented a distinct approach, proposing a graphical solution for the minimum time problem in styrene polymerization.

Due to the unique dynamic of the PBL emulsion polymerization process, the time at which the reactor pressure begins to drop must be also considered when calculating the time-optimal temperature profile (see Chapter 3.3 for details). The minimum batch time problem for this research is a trade-off situation between finding the minimum batch time (t_f) and keeping the reactor pressure under the pressure limitation. The MAWP (Maximum Allowable Working Pressure) for this research is chosen to be 10bar [25]. The reactor temperature set point for the 1st isothermal stage of the three-stage heating process is fixed at 343K, and the maximum operation temperature is set to 353K due to safety issues. The remaining variables of the minimum batch time problem are shown below (see Figure 5-1 and Table 5-1). Figure 5-1 shows the original three-stage heating progress published by LG process [1]. The t_1 in the Figure 5-1 indicates the end of the

doi:10.6342/NTU202402858

first isothermal stage of the three-stage heating progress, which is also the time when the process needs to be heated up to the second reactor temperature set point. The t_2 in the Figure 5-1 indicates the end of the second isothermal stage, and it is also the time when the process needs to be heated up to the third reactor temperature set point. The t_f in the Figure 5-1 indicates the end time for the batch process, which is also the total operation time.

Figure 5-2 shows the results of the first batch operation conducted with two different batch times: 1800 minutes and 1700 minutes (total batch duration). One can see that there is a limitation in achieving the minimum desired value of t_1 under the constraint of the Maximum Allowable Working Pressure (MAWP).

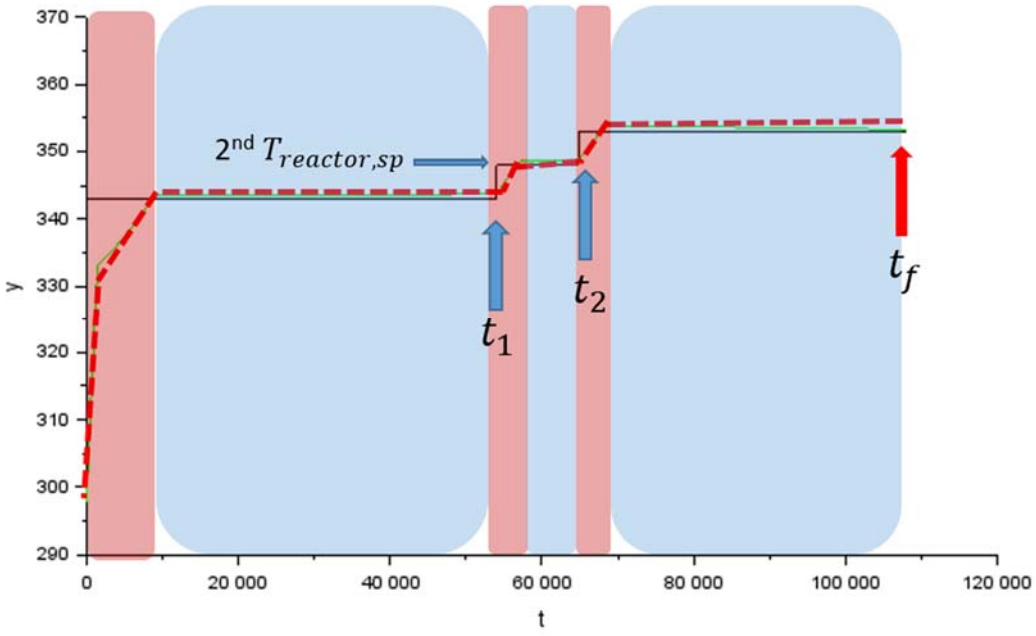

Figure 5-1 Demonstration of the variables of the minimum batch time problem

Table 5-1 Variables of the minimum batch time problem

Variables	Definition

doi:10.6342/NTU202402858

t_1	First heating time point [min]
t_2	Second heating time point [min]
t_f	Total batch time [min]
2nd $T_{reactor,sp}$	Reactor temperature set point of the second isothermal stage [K]

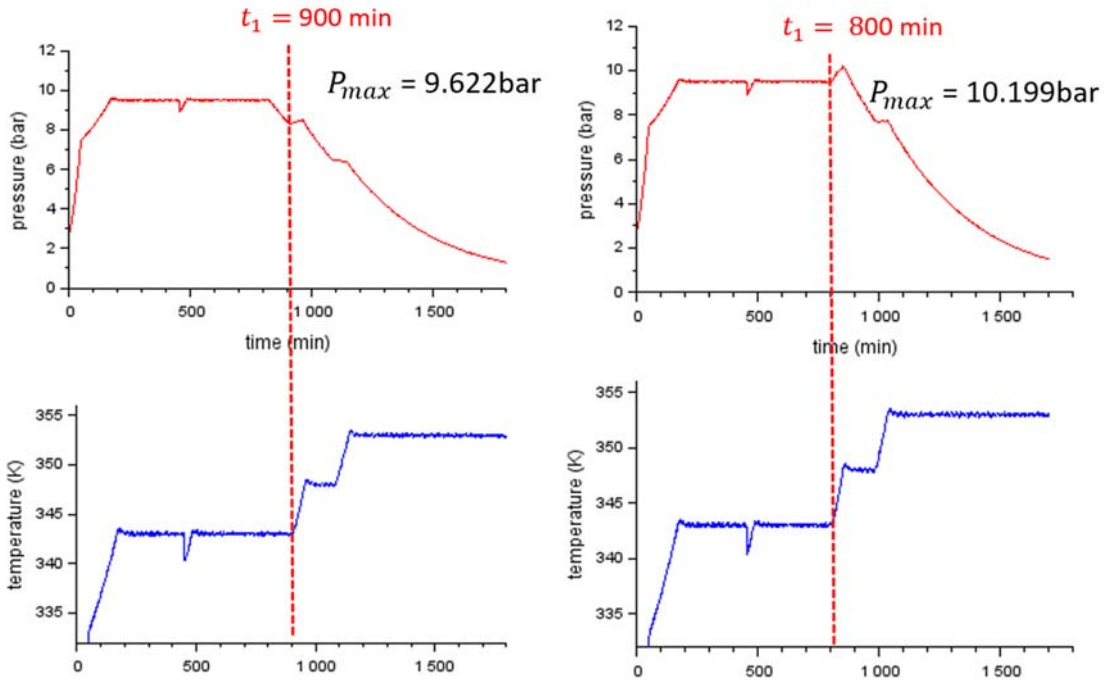

Figure 5-2 Demonstration of the trade-off situation between batch time and P_{max}

The calculated minimum batch time is only valid if it achieves the desired overall conversion of the monomer. The specific value of the desired overall monomer conversion is determined from the results of the first batch operation with the original 1800 minutes batch time of the LG process [1]. The initial batch serves as a reference point because it does not have uncontrollable temperature overshoot caused by polymer fouling issues that may occur in subsequent batches.

Real-time monitoring of aqueous phase monomer concentration is impractical in real plant operation. Therefore, reactor pressure measurement serves as the most viable method to determine when to terminate the operation so as achieve the desired final

doi:10.6342/NTU202402858

conversion. This approach is effective because elevated reactor pressure is mostly caused by the presence of butadiene monomer [4] in the vapor.

Figure 5-3 presents the key results from the first batch operation: final monomer conversion and the corresponding reactor pressure ($X_{m,final} = 0.9677$ and $P_{final} = 1.289\text{bar}$). This initial batch serves as a reference point for future optimizations: the operation should be terminated when reactor pressure drops to around 1.3 bar and the final monomer conversion should be about 0.967.

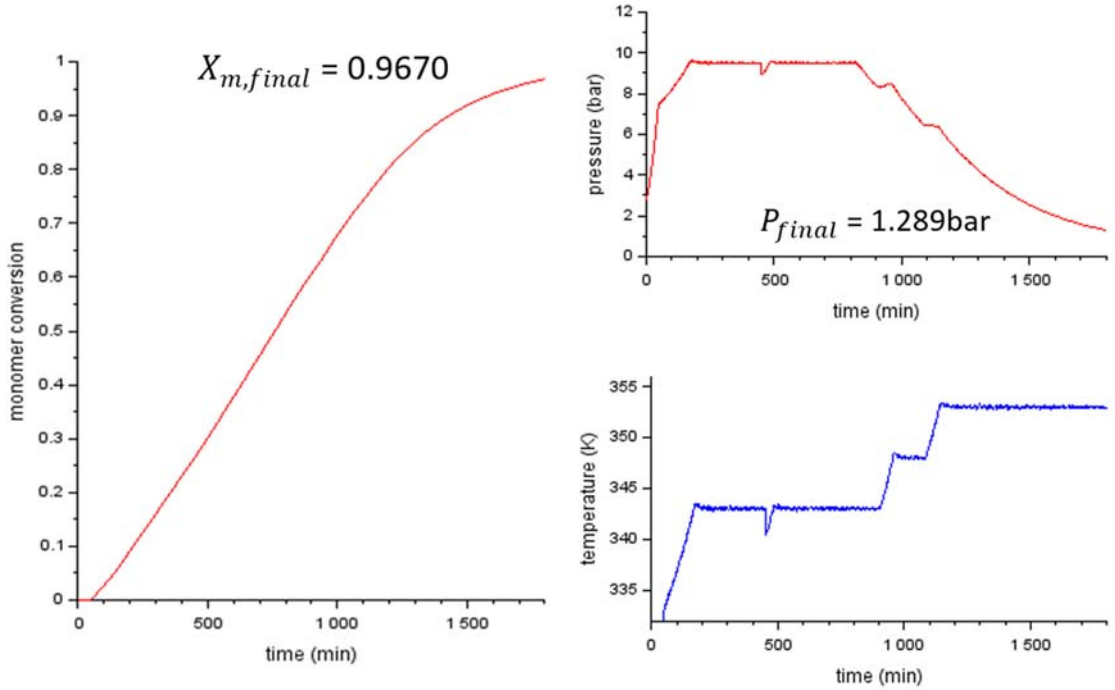

Figure 5-3 1st Batch Performance: Three-Stage Heating (Batch Time = 1800mins)

This study employs a simple exhaustive search algorithm to identify the minimum batch time for the process. The optimization initially considers a three-stage heating profile. Subsequently, a two-stage heating profile will be evaluated for comparison, investigating the impact on the resulting optimal batch time. To simplify the optimization process, the duration of the second isothermal stage in the three-stage profile is fixed at 120 minutes.

doi:10.6342/NTU202402858

5.1.1 Three-Stage Heating Progress

Figure 5-4 shows the optimal batch time for the three-stage profile, as the value of t_1 is approached to minimum, the duration of the third isothermal stage ($t_f - t_2$) needs to be longer to achieve the desired final monomer conversion. The optimal result is 1765 minutes, which saves 35 minutes compared to the original profile.

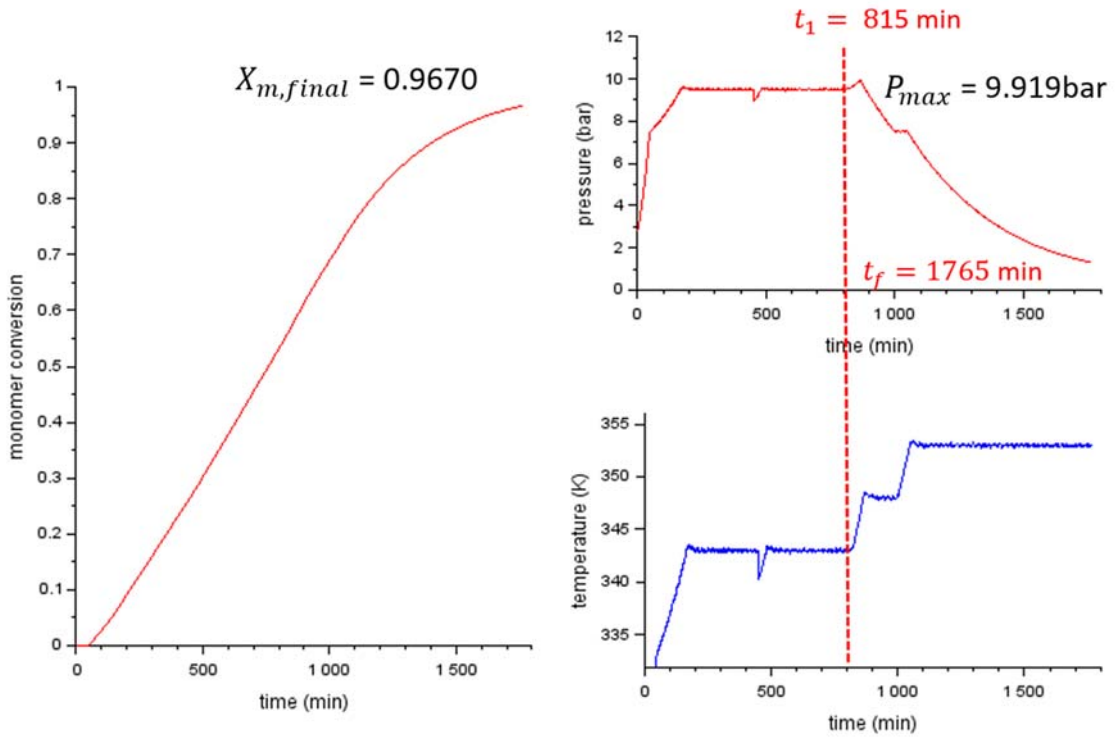

Figure 5-4 1st Batch Performance: Three-Stage Heating (Optimal Batch Time)

Table 5-2 Optimal three-stage profile heating progress

Progress	Temperature (K)	Time duration
1st heating stage (steam)	298 K → 333 K	1.5 hours
1st heating stage (reaction heat)	333 K → 343 K	1.5 hours

doi:10.6342/NTU202402858

1st isothermal stage	343 K	10.6 hours
2nd heating stage	343 K → 348K	1 hour
2nd isothermal stage	348 K	2 hours
3rd heating stage	348 K → 353 K	1 hour
3rd isothermal stage	353 K	11.8 hours

5.1.2 Two-Stage Heating Progress

Figure 5-5 shows the optimal batch time for the two-stage profile, which the two-stage heating process is simply remove the second stage in the three-stage profile by immediately rise up the reactor temperature set point from 343K to 353K. Because of the step change of the reactor temperature set point increase from 5K to 10K compare to the three-stage profile, hence the duration of the first isothermal stage need to be longer than in the three-stage profile in order to satisfy the constraint of the MAWP. The optimal result is 1750 minutes, which saves 50 minutes compared to the original profile.

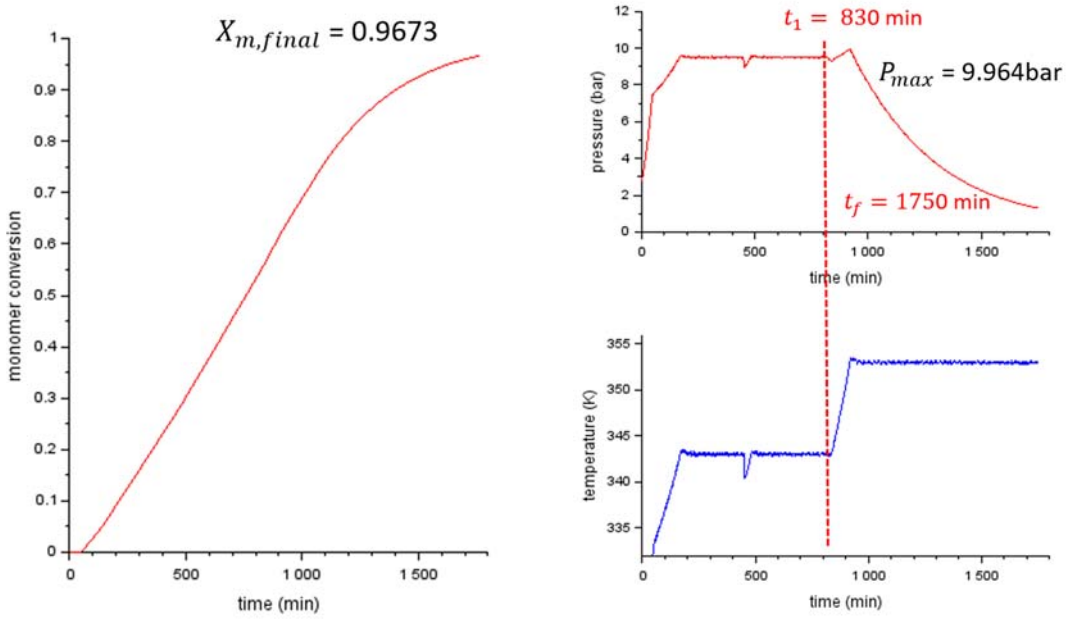

Figure 5-5 Batch Performance: Two-Stage Heating (Optimal Batch Time)

doi:10.6342/NTU202402858

Table 5-3 Optimal two-stage profile heating progress

Progress	Temperature (K)	Time duration
1st heating stage (steam)	298 K → 333 K	1.5 hours
1st heating stage (reaction heat)	333 K → 343 K	1.5 hours
1st isothermal stage	343K	10.8 hours
2nd heating stage	343 K → 353 K	1.5 hour
2nd isothermal stage	353 K	13.9 hours

The results demonstrate that a two-stage heating profile can achieve a shorter batch time compared to the three-stage approach, translating to improved economic efficiency. However, it is important to be aware that the two-stage profiles requires a larger step change in the reactor temperature set point, which presents a greater challenge in maintaining the safe reactor pressure in real plant operation.

5.2 Optimal Controller Tuning Parameters

Unlike continuous processes, batch processes are inherently dynamic and have no steady state. This means variables like process gain and time constants constantly change, often within a wide range throughout a single batch cycle.

These dynamic characteristics make it difficult to control batch processes effectively using traditional linear controllers. Linear controllers are typically good at maintaining precise control within a narrow range, but not the wide operating range encountered in batch processes. Linear controllers employed in batch processes may require parameter scheduling so that tuning parameters change during a batch cycle. This strategy aims to

doi:10.6342/NTU202402858

optimize the closed-loop response across the entire operating range while ensuring stability and avoiding control issues [26][27].

For real plant operation, it is impractical and time-consuming to retune the controllers each time the process dynamic changes. As the emulsion polymerization process itself has time-varying, multi-phase reactions, the batch process variables also exhibit strong temporal correlation. The dynamics change with time during the batch, and there is also often considerable variance between batches due to varied conditions [28].

For this research, the simulation model assumes identical initial conditions, raw material recipes, and batch durations across all simulated batches. The model specifically focuses on incorporating the impact of polymer fouling issue across different batches (see Section 3.4 for details).

This work will first focus on optimizing the primary controller parameters across different batches. Subsequently, the optimization of the primary controller parameters within a single batch cycle will be analyzed and discussed.

The optimization of the controller parameters across different batches will be performed for the optimal two-stage profile developed in Section 5.1.2 and evaluated using a performance index, which is the Mean Absolute Error (MAE) between the reactor temperature and its set point. To calculate the MAE, sampling points will be collected from the moment that the controllers are in action (see Equation 5-1 and Figure 5-6).

$$\mathrm{MAE} = \frac{\sum \left| T_r - T_{r,\mathrm{sp}} \right|}{N} \qquad 5\text{-}1$$

Here N is the number of sampling points.

doi:10.6342/NTU202402858

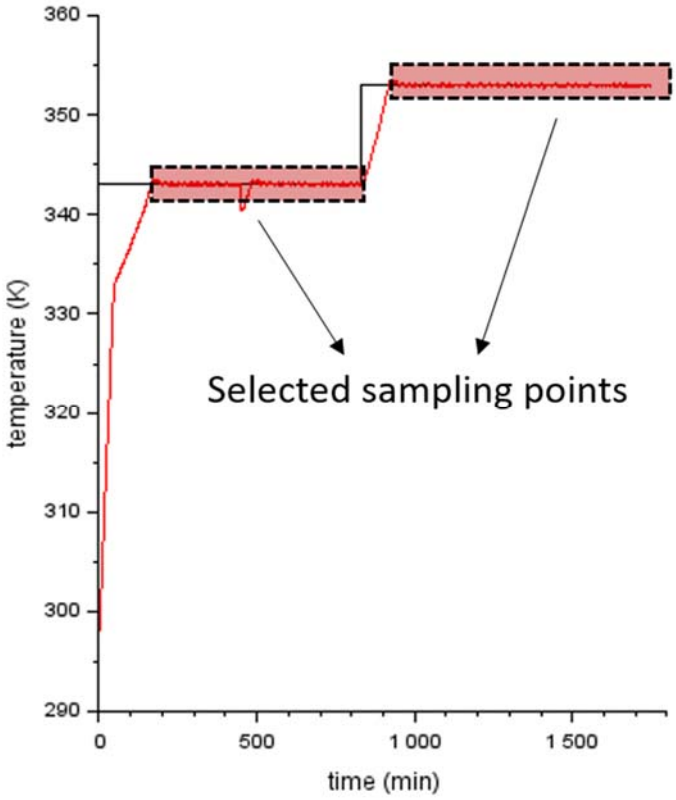

Figure 5-6 Demonstration of the regions where sampling points are collected for determining the MAE

The reason for selecting these two specific regions to calculate the MAE is to avoid the time periods where the controllers are not in action, which is the time before the reactor reaches the desired set point (see 1.2 for details).

Figure 5-7 and Figure 5-8 show the corresponding reactor temperature and the refrigerant level trajectories of the 1st, 20th, 30th and 40th batch operations. The refrigerant level is measured using a linear sensor, where a saturation point of 100% corresponds to a measurement height of 0.74 meters. Analysis of the trajectories reveals very similar process dynamics for the first 30 batches, suggesting good control is possible with a single set of PI parameters. However, as polymer fouling accumulates, the dynamics deviate beyond the 30th batch. Saturation of the controller leads to a loss of control over

doi:10.6342/NTU202402858

temperature and overshoot. Therefore the reactor should be cleaned after around 40 batches.

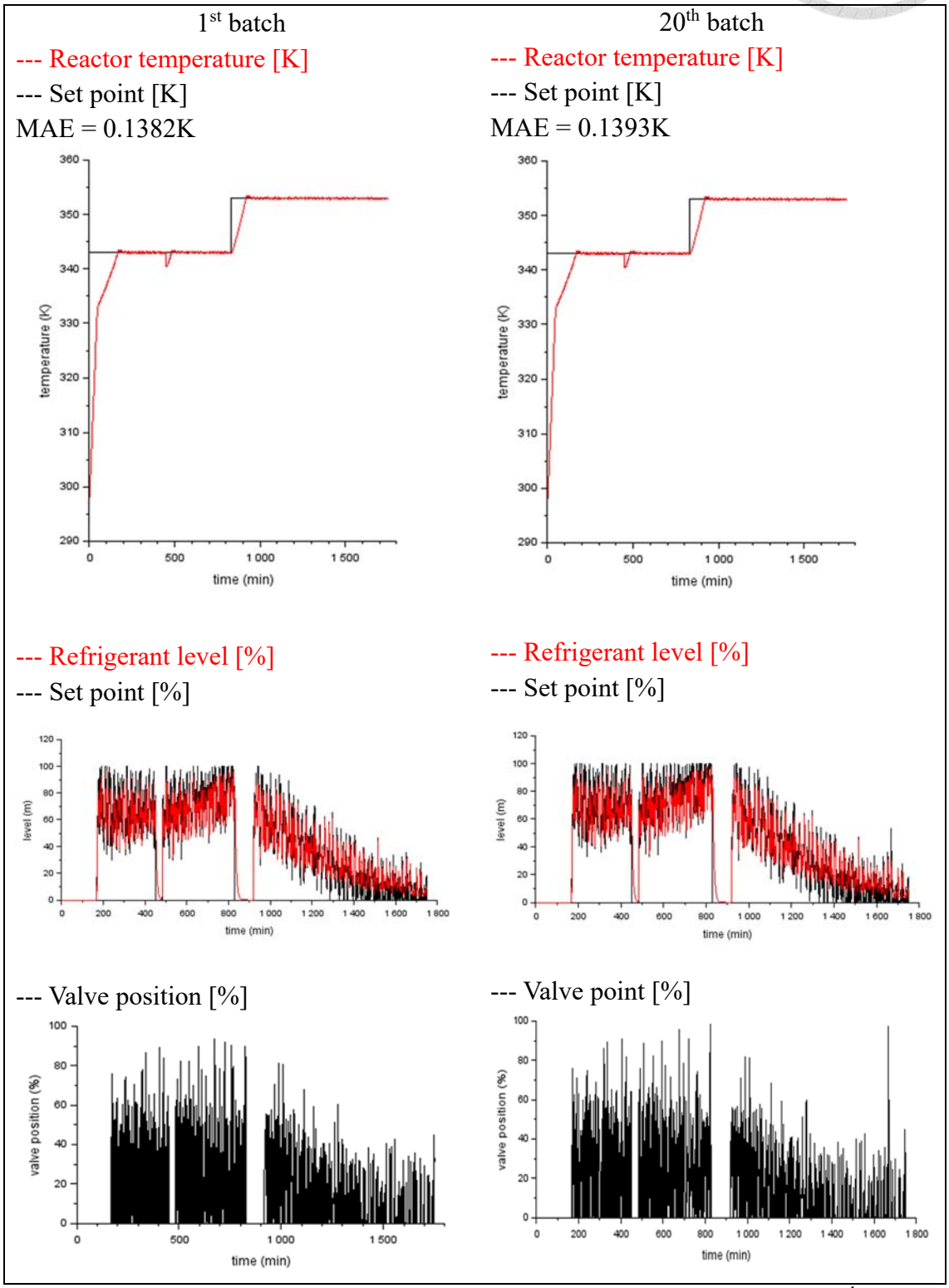

Figure 5-7 Reactor temperature and refrigerant level trajectories of 1st and 20th batch

doi:10.6342/NTU202402858

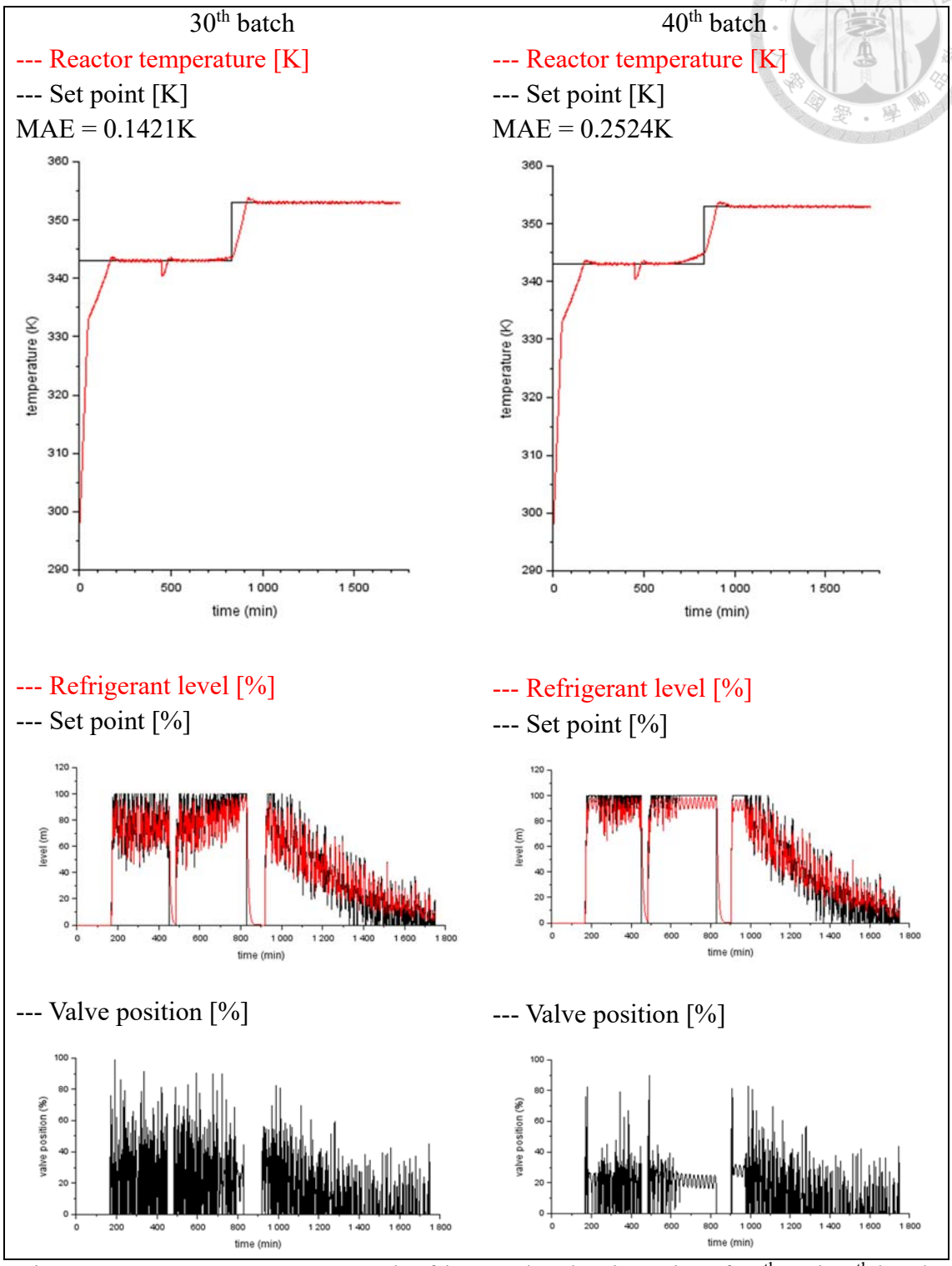

Figure 5-8 Reactor temperature and refrigerant level trajectories of 30th and 40th batch

An exhaustive search method is applied to determine the optimal controller tuning

doi:10.6342/NTU202402858

parameters. This will involve iteratively optimizing the controller gain K_c followed by the integral time constant τ_I (each step for K_c is 0.1 $\frac{\%}{\%}$ and for τ_I is 1 minute). Table 5-4 shows the comparison between the optimal and the original controller parameters ($K_c = 1$ $\frac{\%}{\%}$ and τ_I = 20 minutes) of different batch.

Table 5-4 Comparison between the original and optimal PI parameters

Batch number		K_c ($\frac{\%}{\%}$)	τ_I (min)	MAE (K)	$X_{m,final}$
1st	original	1	20	0.1382	0.9673
	optimal	1.3	15	0.1356	0.9672
20th	original	1	20	0.1393	0.9674
	optimal	1.4	13	0.1362	0.9673
30th	original	1	20	0.1421	0.9674
	optimal	1.5	13	0.1388	0.9673
35th	original	1	20	0.1556	0.9676
	optimal	1.8	13	0.1533	0.9675
40th	original	1	20	0.2524	0.9684
	optimal	1.8	10	0.2406	0.9682

The results of controller parameter optimization indicate a need for increasingly aggressive control strategies as polymeric fouling accumulates, altering process dynamics and impacting reactor temperature control.

The next optimization step involves analyzing dynamic variations within one batch. Mean Absolute Error (MAE) between reactor temperature and its setpoint will be calculated across the two isothermal stages of the current operation (see Figure 5-9 and

doi:10.6342/NTU202402858

Table 5-5). This analysis will determine the necessity of using gain scheduling within a single batch operation.

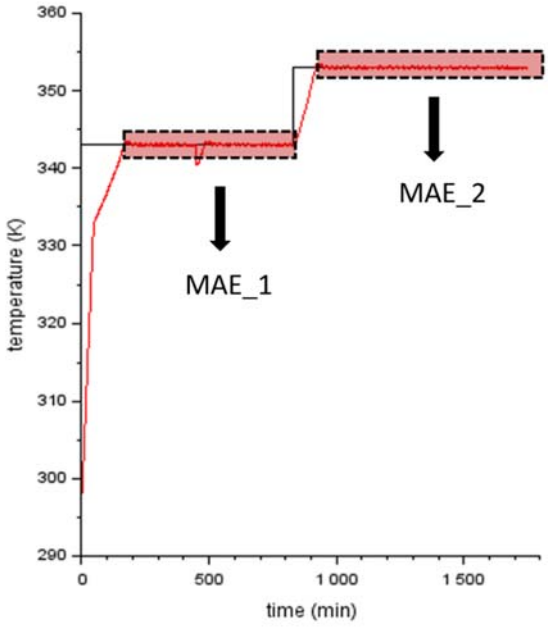

Figure 5-9 Demonstration of the selected sampling points to calculate two different MAE

Table 5-5 MAE of two isothermal stages with optimal controller parameters

Batch number	K_c ($\frac{\%}{\%}$)	τ_I (min)	MAE_1 (K)	MAE_2 (K)	MAE_avg
1st	1.3	15	0.1710	0.1002	0.1356
20th	1.4	13	0.1713	0.1011	0.1362
30th	1.5	13	0.1751	0.1025	0.1388
35th	1.8	13	0.1997	0.1069	0.1533
40th	1.8	10	0.3746	0.1066	0.2406

Table 5-5 shows the calculated Mean Absolute Error (MAE), where the MAE_1 and MAE_2 is the MAE of the first and second plateau shown in Figure 5-9, the MAE_avg is

doi:10.6342/NTU202402858

the average of MAE_1 and MAE_2. The results suggest that the PI controller parameters determined for the first isothermal stage are effective for the second isothermal stage, as the MAE_2 value exhibits minimal variation across batches.

As expected, the step change implemented in the first isothermal stage (see Section 4.2) leads to a higher MAE_1 compared to MAE_2. The observed difference of approximately 0.07K between MAE_1 and MAE_2 from batches 1 to 30 is consistent and indicates the effective controller performance. While a significant increase in MAE_1 is observed for batches 35 and 40, this is likely due to polymeric fouling reducing the overall heat transfer coefficient in the heat exchanger tubes. This decrease in heat transfer efficiency pushes the controller towards saturation, resulting in the observed increase in MAE_1. However, retuning the controller at this stage would be ineffective in improving performance. The current controller settings are already operating at their maximum capacity due to the limitations imposed by the reduced heat transfer.

doi:10.6342/NTU202402858

Chapter 6 Concluding Remarks and Future Works

6.1 Concluding Remarks

In this research project a first-principles model that can capture the approximate process dynamics of the real-plant operation of the polybutadiene latex (PBL) emulsion polymerization batch process was developed. The model, built using ordinary differential equations, can track key process variables such as monomer conversion, temperature, pressure, liquid level, reaction heat generation, and valve position.

Based on this model, further process optimization and analysis are performed. Two different reactor temperature profiles are proposed and compared to improve process productivity. Based on the optimal profile, different sets of controller parameters (K_c and τ_I) of the primary PI controller within the current control structure are tested and optimized across different batches. Conclusions of this research can be summarized as follows:

1. A model has been developed to predict both latex properties and process variables for PBL within a specific batch reactor originally proposed by Yeo et al. [1]. The reactor temperature of this specific batch process is controlled by manipulating the liquid ammonia level within the heat exchange tubes.
2. To simulate real-plant operation more accurately, the model incorporates process noise. The noise accounts for potential variations in measurements like temperature, liquid level, valve position, and reaction heat generation. Sensitivity analysis revealed that temperature measurement noise has the most significant impact on the process.
3. To capture the dynamic variations within a single batch and across different

doi:10.6342/NTU202402858

batches, the model incorporates equations that describe the viscosity and polymeric fouling issues of the PBL batch process.

4. To enhance the process productivity, this work not only optimized the original reactor temperature profile but also proposed and optimized a different profile with only two isothermal stages. Simulations revealed that this profile can reduce the batch time by approximately 50 minutes.
5. The study investigated the retuning and parameters scheduling of the primary PI controller of the PBL process. While the optimization did not significantly improve control results in the short term, it revealed a key finding. As the overall heat transfer coefficient decreases due to viscosity and polymeric fouling, the temperature control will be limited by the saturation of the heat exchange tubes (the saturation issues happen around 35^{th} to 40^{th} batch operation), hence the control performance will not be significantly improved by simply changing the control strategy.

6.2 Future Works

1. Due to the inherent complexity of the emulsion polymerization mechanism, many assumptions (see 3.6) were made during the model development. While these assumptions are helpful for simplifying the mathematical model, they also limit the model's ability to perfectly replicate real-plant dynamics. To simulate the more realistic model response, more complicated methods and theories should be employed such as collision theory for describing the particle nucleation [5], diffusion-based approach to radical capture [29], free-volume theory for diffusion-controlled propagation and termination stage [30][31] and

doi:10.6342/NTU202402858

the polydispersity of the particle size [32][33].

2. Current understanding of the optimal reactor temperature profile may be incomplete. Further investigation is needed to explore potentially superior profiles with multi-stage heating (e.g., four or five stages) for improved reaction control and efficiency. Also, reducing the number of heating stages could lead to unexpected temperature and pressure overshoot, potentially violating the MAWP and desired product quality [34].
3. The optimal parameters scheduling for the secondary controller of the current control structure should also be investigated. This controller can also influence the process dynamics, analyzing and optimizing its settings may help improve the overall control performance and stability.

doi:10.6342/NTU202402858

REFERENCE

[1] Yeo, Y.-K.; Kwon, T.-I.; Lee, K. H. An energy effective PID tuning method for the control of polybutadiene latex reactor based on closed-loop identification. *Korean Journal of Chemical Engineering* **2004**, *21* (5), 935-941. DOI: 10.1007/BF02705574.

[2] Condon, F. E. "Influence of temperature of polymerization on the structural composition of emulsion polymers of butadiene." *Journal of Polymer Science* 11.2 (1953): 139-149.

[3] Pires, N. M., Coutinho, F. M., & Costa, M. A. (2004). Synthesis and characterization of high cis-polybutadiene: influence of monomer concentration and reaction temperature. *European polymer journal*, *40*(11), 2599-2603.

[4] Meehan, E., Variation of Monomer Pressure with Degree of Conversion in Emulsion Polymerization of Butadiene and of Butadiene--Styrene. Journal of the American Chemical Society, 71(2), 628-633, 1949

[5] Washington, I. D. (2008). *Dynamic modelling of emulsion polymerization for the continuous production of nitrile rubber* (Master's thesis, University of Waterloo).

[6] Soroush, M., & Kravaris, C. (1992). Nonlinear control of a batch polymerization reactor: an experimental study. *AIChE journal*, *38*(9), 1429-1448.

[7] Takamatsu, T., Shioya, S., Okada, Y., & Uchiyama, M. (1987). Application of an Adaptive Controller to Molecular Weight Distribution Control in a Batch Polymerization Process. *IFAC Proceedings Volumes*, *20*(5), 227-232.

[8] Chylla, R. W., & Haase, D. R. (1993). Temperature control of semibatch polymerization reactors. *Computers & Chemical Engineering*, *17*(3), 257-264.

doi:10.6342/NTU202402858

[9] Soroush, M., & Kravaris, C. (1992). Nonlinear control of a batch polymerization reactor: an experimental study. *AIChE journal*, *38*(9), 1429-1448.

[10] Chern, C. S. (2006). Emulsion polymerization mechanisms and kinetics. *Progress in polymer science*, *31*(5), 443-486.

[11] Harkins, W. D. (1945). A general theory of the reaction loci in emulsion polymerization. *The Journal of chemical physics*, *13*(9), 381-382.

[12] Harkins, W. D. (1946). A general theory of the reaction loci in emulsion polymerization. II. *The Journal of Chemical Physics*, *14*(1), 47.

[13] Harkins, W. D. (1947). A general theory of the mechanism of emulsion polymerization1. *Journal of the American Chemical Society*, *69*(6), 1428-1444.

[14] Smith, W. V., & Ewart, R. H. (1948). Kinetics of emulsion polymerization. *The journal of chemical physics*, *16*(6), 592-599.

[15] Smith, W. V. (1948). The kinetics of styrene emulsion polymerization1a. *Journal of the American Chemical Society*, *70*(11), 3695-3702.

[16] Smith, W. V. (1949). Chain initiation in styrene emulsion polymerization. *Journal of the American Chemical Society*, *71*(12), 4077-4082.

[17] Fitch, R. M., & Tsai, C. H. (1971). Particle formation in polymer colloids, III: Prediction of the number of particles by a homogeneous nucleation theory. In *Polymer Colloids: Proceedings of an American Chemical Society Symposium on Polymer Colloids held in Chicago, Illinois, September 13–18, 1970* (pp. 73-102). Boston, MA: Springer US.

[18] Fitch, R. M., & Tsai, C. H. (1969, January). Homogeneous nucleation of polymer colloids. In *Proceedings of the National Academy of Sciences of the United States of America* (Vol. 64, No. 4, p. 1424). 2101 CONSTITUTION AVE NW, WASHINGTON, DC 20418: NATL ACAD SCIENCES.

doi:10.6342/NTU202402858

[19] Fitch, R. M. (1973). The homogeneous nucleation of polymer colloids. *British polymer journal*, *5*(6), 467-483.

[20] Vega, J. R., Gugliotta, L. M., Bielsa, R. O., Brandolini, M. C., & Meira, G. R. (1997). Emulsion copolymerization of acrylonitrile and butadiene. Mathematical model of an industrial reactor. *Industrial & engineering chemistry research*, *36*(4), 1238-1246.

[21] Sacks, M. E., Lee, S. I., & Biesenberger, J. A. (1973). Effect of temperature variations on molecular weight distributions: batch, chain addition polymerizations. *Chemical Engineering Science*, *28*(1), 241-257.

[22] Masterson, P. M. (1977). *The time-optimal control of a batch polymerization system* (Doctoral dissertation, University of Colorado at Boulder).

[23] Chen, S. A., & Jeng, W. F. (1978). Minimum end time policies for batchwise radical chain polymerization. *Chemical Engineering Science*, *33*(6), 735-743.

[24] Wu, G. Z. A., Denton, L. A., & Laurence, R. L. (1982). Batch polymerization of styrene-optimal temperature histories. *Polymer Engineering & Science*, *22*(1), 1-8.

[25] API RP520, Sizing, Selection, and Installation of Pressure-Relieving Devices in Refineries, American Petroleum Institution, 2000

[26] Juba, M. R., & Hamer, J. W. (1986). Progress and challenges in batch process control. *proceedings of the CPC III, CHACE*.

[27] MacGregor, J. F. (1988). Control of polymerization reactors. In *Dynamics and Control of Chemical Reactors and Distillation Columns* (pp. 31-35). Pergamon.

[28] Wang, K., Rippon, L., Chen, J., Song, Z., & Gopaluni, R. B. (2019). Data-driven dynamic modeling and online monitoring for multiphase and multimode batch processes with uneven batch durations. *Industrial & Engineering Chemistry*

doi:10.6342/NTU202402858

Research, *58*(30), 13628-13641.

[29] Gao, J., & Penlidis, A. (2002). Mathematical modeling and computer simulator/database for emulsion polymerizations. *Progress in polymer science*, *27*(3), 403-535.

[30] Broadhead, T. O. (1984). *Dynamic modelling of the emulsion copolymerization of styrene/butadiene* (Doctoral dissertation).

[31] Gao, J., & Penlidis, A. (2002). Mathematical modeling and computer simulator/database for emulsion polymerizations. *Progress in polymer science*, *27*(3), 403-535.

[32] Broadhead, T. O., Hamielec, A. E., & MacGregor, J. F. (1985). Dynamic modelling of the batch, semi-batch and continuous production of styrene/butadiene copolymers by emulsion polymerization. *Die Makromolekulare Chemie: Macromolecular Chemistry and Physics*, *10*(S19851), 105-128.

[33] Penlidis, A. (1986). *Polymer reactor design, optimization and control in latex production technology* (Doctoral dissertation).

[34] Hu, K. H., Kao, C. S., & Duh, Y. S. (2008). Studies on the runaway reaction of ABS polymerization process. *Journal of hazardous materials*, *159*(1), 25-34.

[35] Weerts, P. A., Van der Loos, J. L., & German, A. L. (1991). Emulsion polymerization of butadiene, 3. Kinetic effects of stirring conditions and monomer/water ratio. *Die Makromolekulare Chemie: Macromolecular Chemistry and Physics*, *192*(9), 1993-2008.

[36] Haar, L., & Gallagher, J. S. (1978). Thermodynamic properties of ammonia. *Journal of Physical and Chemical Reference Data*, *7*(3), 635-792.

[37] Ilie, A., Girip, A., Calotă, R., & Călin, A. (2022). Investigation on the Ammonia Boiling Heat Transfer Coefficient in Plate Heat Exchangers. *Energies*, *15*(4), 1503.

doi:10.6342/NTU202402858

[38] Heat Exchanger Design Handbook, 1986, by C. F. Beaton.

[39] Dimitratos, J., Georgakis, C., El-Aasser, M. S., & Klein, A. (1989). Dynamic modeling and state estimation for an emulsion copolymerization reactor. *Computers & chemical engineering*, *13*(1-2), 21-33.

[40] McCabe, Warren L. (Warren Lee), 1899-1982. (2001). Unit operations of chemical engineering. Boston :McGraw Hill.

[41] Xiao, M., Tang, L., Zhang, X., Lun, I. Y. F., & Yuan, Y. (2018). A review on recent development of cooling technologies for concentrated photovoltaics (CPV) systems. *Energies*, *11*(12), 3416.

doi:10.6342/NTU202402858

APPENDICES

A. Valve characteristic

The valve characteristic is given by the following equation (see Equation A-1), for equal percentage valve $f(x) = e^{k(x-1)}$ [40](e^k is constant, set as 50 for globe valve).

After some simple derivations, can get the equation for describing the valve characteristic (see Equation A-2).

The visualization of the volumetric flow rate varying with valve position from 0 to 1 is given in the following figure (see Figure A-1)

$$q = C_v(x)\sqrt{\frac{\Delta p}{\rho}} = C_{v,max} * f(x)\sqrt{\frac{\Delta p}{\rho}} \quad \text{A-1}$$

$$q \cong 21.4984 * (50)^{x-1}\, gpm \cong 0.08138 * 50^{x-1}\frac{m^3}{min}. \quad \text{A-2}$$

$q =$ actual volmetric flow rate through the valve $[gpm,$ gallon per minute]

x : valve position (0~1)

$C_{v,max}$: maximum valve coefficient

ρ : specifc gravity of fluid, rlative to water at 70°F (~ 550 for $NH_{3,liq}$ at 330K)

Δp : differential pressure across the valve (set as constant = 100psi)

doi:10.6342/NTU202402858

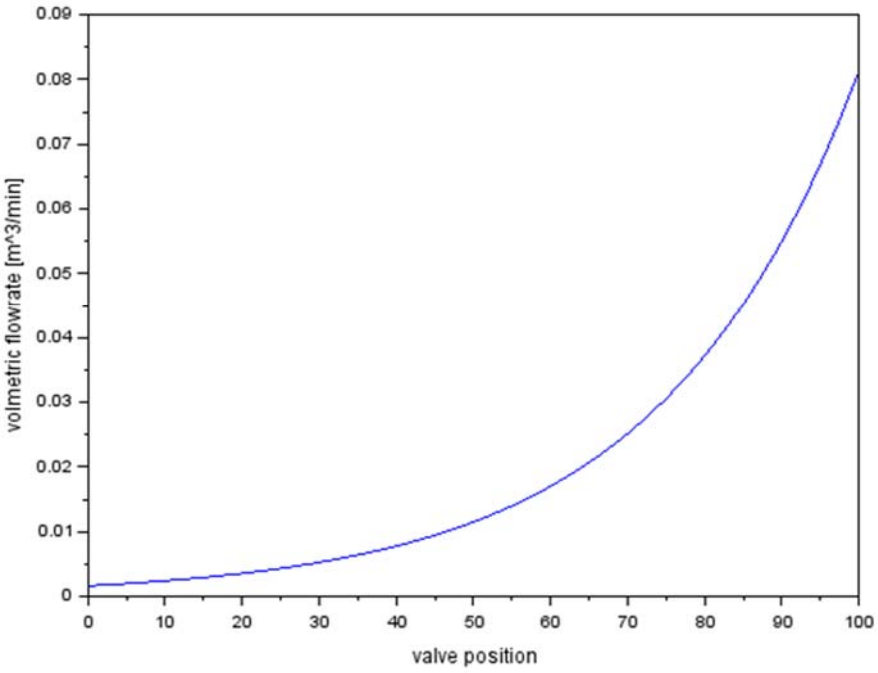

Figure A-1 Valve characteristic (with pressure drop Δp = 100psi)

B. Process diagram

Figure B-2 shows the process diagram developed using the Scilab Xcos simulation environment. The simulation was configured to use minutes as the time unit.

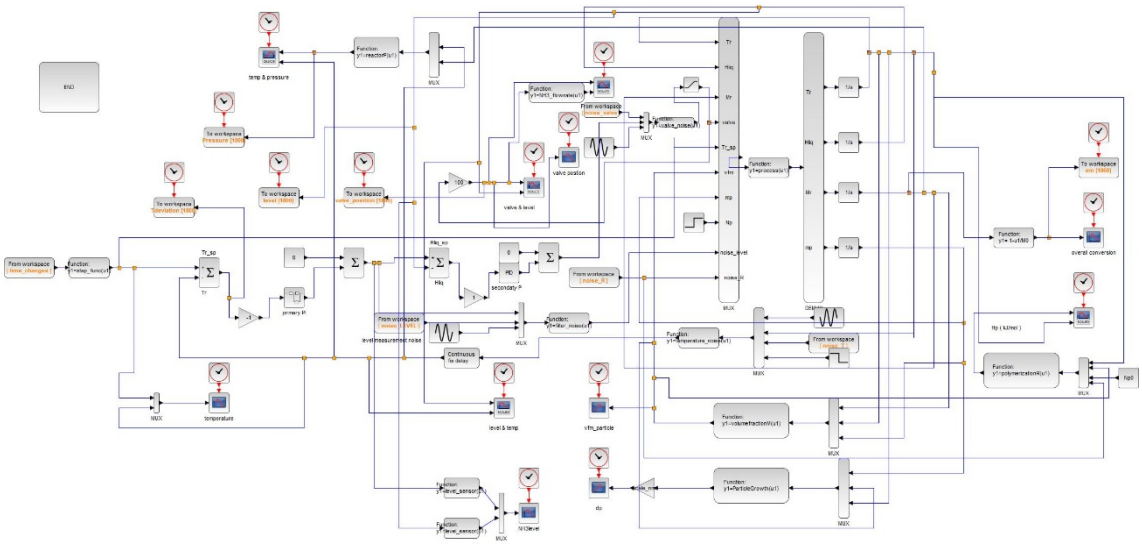

Figure B-2 Xcos process diagram

doi:10.6342/NTU202402858

The PID block provided natively in Xcos was used initially as the feedback controller. Later it was found that this block lacks a reset-windup function which is a critical feature for preventing saturation (see Figure B-3). Consequently, a custom superblock containing a self-built PID block with reset-windup functionality was developed (see Figure B-4).

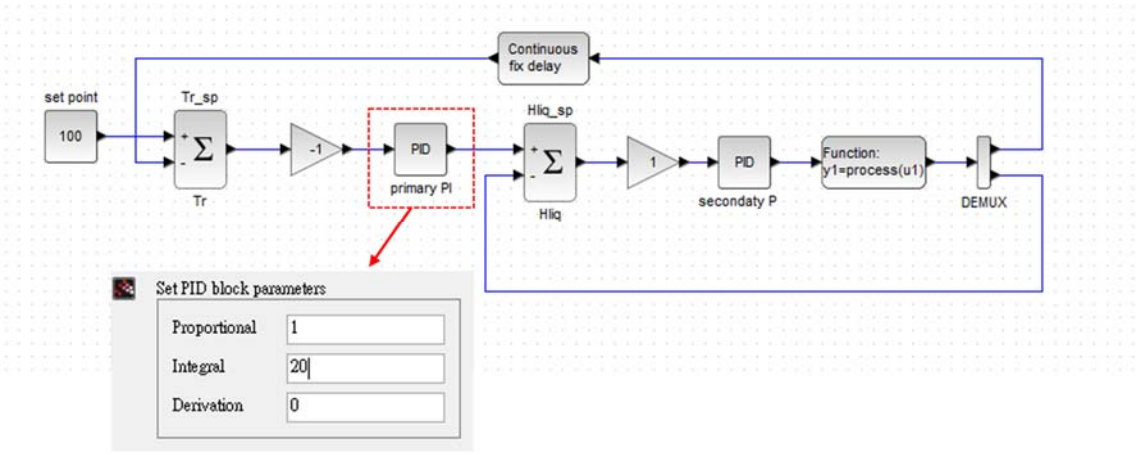

Figure B-3 Demonstration of the original control structure

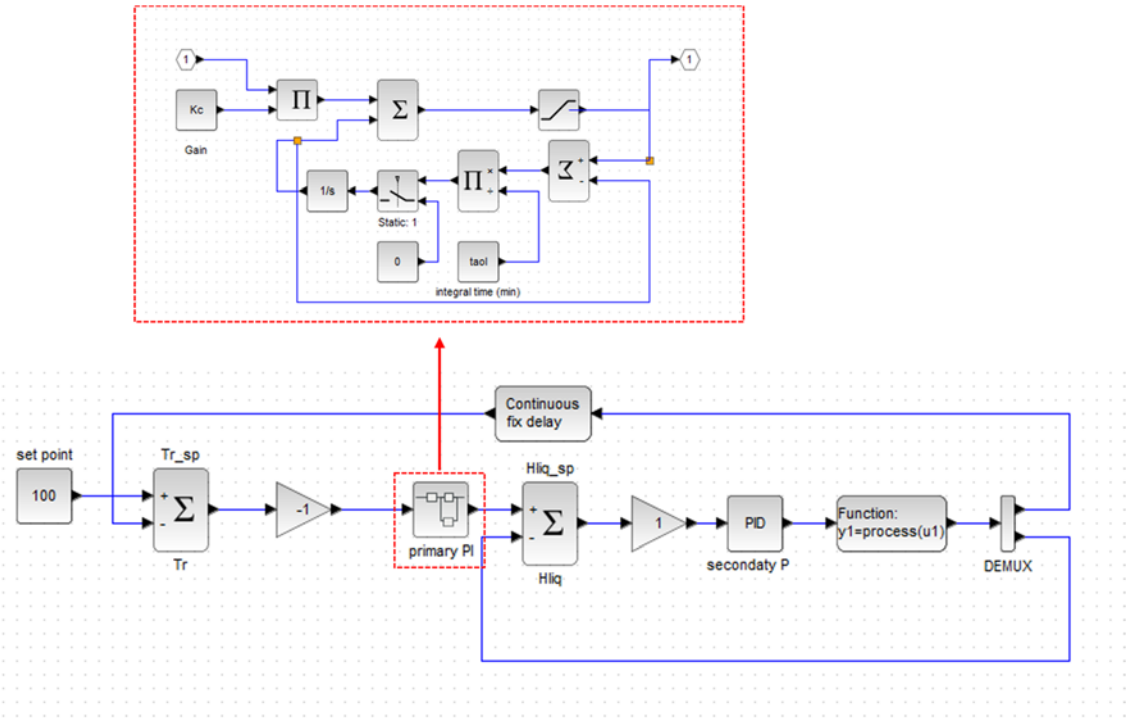

Figure B-4 Demonstration of the modified control structure

doi:10.6342/NTU202402858

The reset-windup function is implemented by a Saturation block and a SWITCH_f block, as the saturated value is reached, the integrating term will be switched to zero (see Figure B-4).

The implementation of the noise is presented as Figure B-5, a self-defined block is implemented into the feedback of the reactor temperature measurement. The self-defined function is written with the Scinotes function built-in Scilab, acting as an summation of all the variables from MUX block, and of course the summation block is provided in Scilab, but using a self-defined function can help us set the magnitude of the corresponding noise more easily during the simulation process.

The fourth input of the MUX block in Figure B-5 is a step change generator with a magnitude of 2.5K at 450 minutes, which is responsible for simulate the unknown disturbance that cause the sudden drop-down of the reactor temperature trajectory in real-plant operation (see Section 4.2 for details).

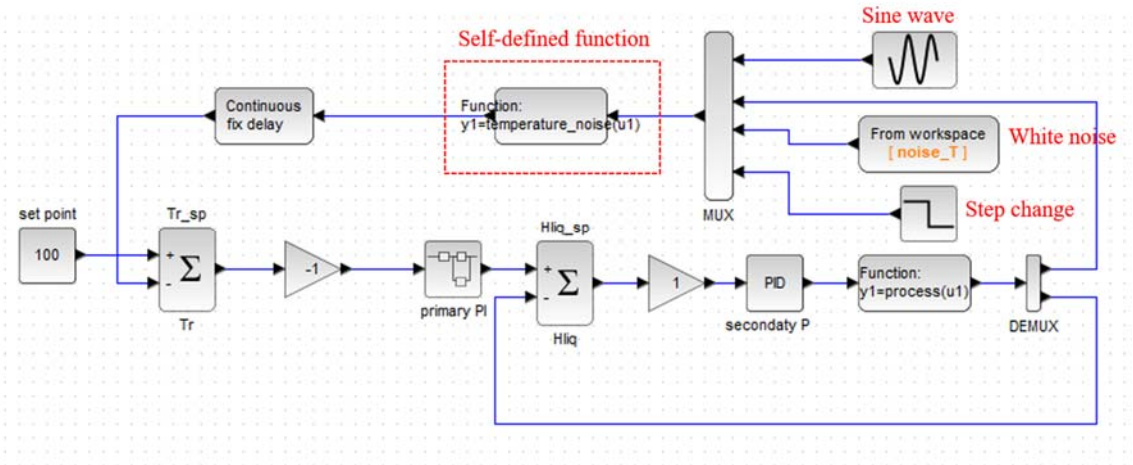

Figure B-5 Demonstration of the implementation of disturbances in temperature measurement

The rand() function is provided in the Scilab environment, which can generates a new set of random numbers with each execution. To ensure consistency in the process

doi:10.6342/NTU202402858

model, generated noise should be saved as external CSV files and then imported into the simulation environment.

C. Model Parameters

Table C-1 Reactor design database items

Item	Value
Shape	Cylindrical
Diameter	1 m
Height	1.304 m
Volume	1 m^3

Table C-2 Heat exchange tubes design database items

Item	Value
Material	Ferritic stainless steel ($k = 26.8\ [\frac{W}{m*K}]$)
Tube type	Schedule40 (¼ inches pipe)
$r_{o,tube}$	$6.85mm$
$r_{i,tube}$	$5.12mm$
Total number of tubes	50
$A_{c,tube}$	$8.236 * 10^{-5}\ m^2$

Table C-3 Recipe of PBL batch process

Component		Reference
water	$580\ kg$	[35]
Butadiene	$253\ kg$	
Emulsifier	$0.01\frac{kmol}{m^3}$	

doi:10.6342/NTU202402858

$(a_s = 1.037 * 10^8 \ \frac{m^2}{kmol})$		
Initiator $(f = 0.7)$	$0.013 \ \frac{kmol}{m^3}$	

Table C-4 Butadiene database items

Item	Value	Reference
k_p	$4.713 \times 10^8 \times e^{\frac{-3.937 * 10^7}{RT}} \ [\frac{1}{s}]$	[5]
k_d	$1.443 \ \times 10^{16} \times e^{\frac{-1.668 * 10^8}{RT}} [\frac{1}{s}]$	
ρ_M	$646 \ - 1.271 \times (T - 273.15) [\frac{kg}{m^3}]$	
ρ_P	$891 \ - 0.025714 \times (T - 273.15) \ [\frac{kg}{m^3}]$	
ρ_P	$-72.73 \ \times 10^4 \frac{J}{mol}$	
x_c	0.55	

Table C-5 Refrigerant ($NH_{3,liq}$) database items

Item	Value	Reference
ρ_{NH_3}	$650 \frac{kg}{m^3}$	[36]
H_{vap}	$17283 \frac{J}{mol}$	
$T_{sat,24.2bar}$	$330K$	
h_{NH_3}	$1377 \sim 3050 \frac{W}{m^2 K}$	[37]

Table C-6 Steam database items

Item	Value	Reference
$T_{4.15atm}$	$418K$	[38]

doi:10.6342/NTU202402858

$C_{p_{steam}}$	$1996\frac{J}{kgK}$	
$H_{v_{steam}}$	$2740\frac{kJ}{kg}$	

D. Steam heating validation

The energy balance equation for calculating the batch reactor temperature is listed as Equation 3-1. The steam heating term is expressed as the following.

$$\text{steam heating} = C_{p_{steam}} \times (T_{steam} - T_{reactor}) + H_{g_{steam}}$$

To ensure the accuracy of our model, it is crucial to validate the term representing steam heating within the energy balance equation. This validation process will verify that the chosen model and its parameters accurately capture the heat transfer dynamics associated with the steam supply.

To validate the steam heating term, the simplified energy balance of the reactor without the reaction and heat exchange tubes is considered as the following.

$$(V_r \times \rho_r \times C_{pr})\frac{dT_r}{dt} = \dot{m}(C_{p,s} \times (T_s - T_r) + H_{g,s})$$

As the first heating progress of the original three-stage profile is entirely by steam heating, we can select this section to do the validation.

doi:10.6342/NTU202402858

The following figure shows the model simulation of the 1st batch operation without the disturbances, noise and measurement delay. From the selected first heating section, it can be seen that the heating from 298K to 333K (the desired reaction temperature) takes about 80 minutes to finish (see Figure D-6 Demonstration of first heating section.

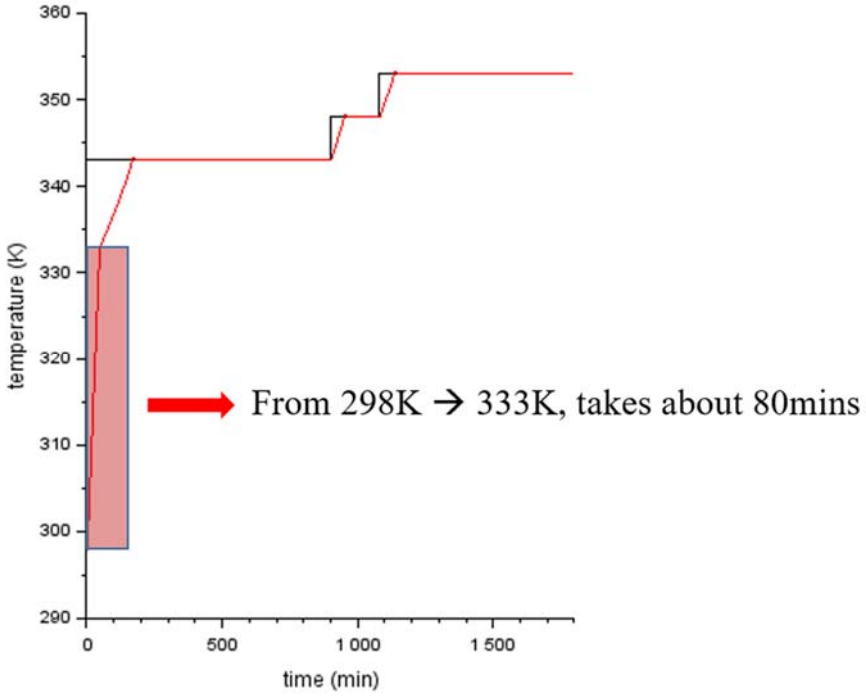

Figure D-6 Demonstration of first heating section

The mass flow rate of the steam supply employed in the model is considered as a constant value with magnitude of $0.6\frac{kg}{min}$, we can then recalculate the corresponding heating time for the reactor temperature rise from 298K to 333K.

$$\frac{dT_r}{dt} = \frac{0.6\ (1996\frac{J}{kg*K}\ *(\ 418K\ - T_r) + 2740\ *10^3\frac{J}{kg}\ )}{1\ m^3\ *1000\frac{kg}{m^3}\ *4000\frac{J}{kg*K}}$$

Integrating this equation numerically from 298K to 333K gives a value of 79 minutes. This is similar to the value from the Xcos simulation which suggests that the model for the steam heating is correct.

doi:10.6342/NTU202402858

E. Overall heat transfer coefficient

The initial value overall heat transfer coefficient of the heat exchange tubes is calculated based on the following correlation.

$$\frac{1}{U_0} = \frac{1}{h_i} + \frac{l}{k} + \frac{1}{h_o}$$

U_0 : initial value of the overall heat transfer of the heat exchange tubes at x_m = 0

h_i : boiling heat transfer coefficient of liquid ammonia, set as $1377 \frac{W}{m^2 * K}$ [37]

h_o : convective heat transfer coefficient of water, set as $600 \frac{W}{m^2 * K}$ [41]

k : conduction heat transfer coefficient of ferretic stainless steel, set as $26.8 \frac{W}{m * K}$ [41]

l : tube thickness, for this model it is 1.73 * 10^{-3}m

$$U_0 = \left(\frac{1}{1377} + \frac{(6.85 - 5.12) * 10^{-3}}{26.8} + \frac{1}{600} \right)^{-1} \cong 407 \frac{W}{m^2 * K}$$

doi:10.6342/NTU202402858